Molecular phenotyping uncovers differences in basic housekeeping functions among closely related species of hares (*Lepus* spp., Lagomorpha: Leporidae)

Running title: Molecular-level species differences among hares

Kateryna Gaertner[1]‡, Craig Michell[2,3]‡, Riikka Tapanainen[2], Steffi Goffart[2], Sina Saari[1], Manu Soininmäki[2], Eric Dufour[1]‡ and Jaakko L. O. Pohjoismäki[2]†‡

†Corresponding author

‡These authors contributed equally

[1]Mitochondrial Bioenergetics and Metabolism, Faculty of Medicine and Health Technology, FI-33014 Tampere University, Finland

[2]Department of Environmental and Biological Sciences, FI-80101 University of Eastern Finland, Finland

[3]Red Sea Research Center, Division of Biological and Environmental Science and Engineering, King Abdullah University of Science and Technology (KAUST), Thuwal, Saudi Arabia

Abstract

Speciation is a fundamental evolutionary process, which results in genetic differentiation of populations and manifests as discrete morphological, physiological and behavioral differences. Each species has travelled its own evolutionary trajectory, influenced by random drift and driven by various types of natural selection, making the association of genetic differences between the species with the phenotypic differences extremely complex to dissect. In the present study, we have used an *in vitro* model to analyze in depth the genetic and gene regulation differences between fibroblasts of two closely related mammals, the arctic/subarctic mountain hare (*Lepus timidus* Linnaeus) and the temperate steppe-climate adapted brown hare (*Lepus europaeus* Pallas). We discovered the existence of a species-specific expression pattern of 1,623 genes, manifesting in differences in cell growth, cell cycle control, respiration, and metabolism. Interspecific differences in the housekeeping functions of fibroblast cells suggest that speciation acts on fundamental cellular processes, even in these two interfertile species. Our results help to understand the molecular constituents of a species difference on a cellular level, which could contribute to the maintenance of the species boundary.

Keywords

speciation; transcriptome; genome; metabolism; mammal; evolution.

Introduction

Species are the central units for taxonomy, evolution and biodiversity research. Species are commonly defined by emphasizing reproductive isolation between them, also known as the biological species concept (Dobzhansky, 1937; Mayr, 1942). Although the concept is not fully comprehensive regarding e.g. asexual organisms or gene flow across species barriers (Abbott et al., 2013; Chan & Levin, 2005; Giska et al., 2019; Hamilton & Miller, 2016; Harrison &

Larson, 2014; Hedrick, 2013; Mallet, Besansky, & Hahn, 2016; Soubrier et al., 2016; Todesco et al., 2016; Wolf, Lindell, & Backstrom, 2010), it remains a valid generalization for most animal species. Species are products of evolutionary processes, which result in genetic differentiation of originally similar populations with common ancestry (Wolf et al., 2010). When given enough time, this differentiation will contribute to the formation of reproductive barriers.

While some part of the genetic differentiation can be attributed to random genetic drift, which operates in all populations and contributes also to the phenotypic differences between isolated populations, natural selection is a much more potent driver of differentiation through local adaptation and specialization (Arnegard et al., 2014; Schluter & Conte, 2009; Wolf et al., 2010). The selective pressures underlying the adaptation to different habitats can be complex and taxon-dependent (MacColl, 2011). From the ecological perspective, successful exploitation of a habitat requires adaptation to both abiotic and biotic factors, including co-evolution with other organisms. Species differences result from combinations of adaptations, each associated with trade-offs (Southwood, 1988).

Two closely related species can hybridize in nature. However, if two species are genetically incompatible or their hybrids maladapted, hybrid zones can form in the contact regions of the two species (Abbott et al., 2013; Adavoudi & Pilot, 2021; Harrison & Larson, 2014), and natural selection can reinforce the reproductive barrier by favoring individuals which avoid pairing with the wrong species. However, the situation can be more complex. For example, in the Nordic countries an expansive species, the brown hare (*Lepus europaeus* Pallas, Lagomorpha: Leporidae), is gradually establishing itself in regions formerly dominated by the mountain hare (*Lepus timidus* Linnaeus). The two species hybridize and produce fertile

offspring, resulting in notable allele sharing, without the formation of hybrid zones (Levanen, Thulin, Spong, & Pohjoismaki, 2018; Pohjoismaki, Michell, Levanen, & Smith, 2021). Similar gene flow has been observed between other, more related members of the *Lepus* genus (Ferreira et al., 2020; Ferreira et al., 2021; Giska et al., 2019; Marques, Farelo, et al., 2017; Melo-Ferreira, Farelo, et al., 2014; Melo-Ferreira, Seixas, Cheng, Mills, & Alves, 2014). Based on mitochondrial DNA (mtDNA) introgression, hybridization between the two hare species occurs mostly unidirectional, specifically between mountain hare females and brown hare males (Levanen, Kunnasranta, et al., 2018; Thulin & Tegelström, 2002). The reasons for this unidirectionality might be related with reproductive behavior (Thulin & Tegelström, 2002), adaptive advantage of residential mtDNA haplotypes (Melo-Ferreira et al., 2005; Melo-Ferreira et al., 2007) or demographic factors causing genetic drift at the leading edge of the range expansion (Alves, Melo-Ferreira, Freitas, & Boursot, 2008; Ferreira et al., 2021; Marques, Farelo, et al., 2017).

The relatively free gene flow between the two species is remarkable as mountain hare and brown hare are separated by about three million years of evolution (Ferreira et al., 2021). In fact, mountain hares are more related to North American hare species such as white-tailed jackrabbit (*Lepus townsendii* Bachman) than to brown hares, whose closest relatives are the Near Eastern/African cape hare (*Lepus capensis* L.) and Ethiopian hare (*Lepus fagani* Thomas) (Ferreira et al., 2021). It is likely that the mountain hare has its evolutionary origin in the Beringian or Nearctic region whereas the brown hare lineage likely originates from the southern Palearctic or Ethiopian biogeographic realm.

The mountain hare is an arctic/subarctic tundra to taiga forest specialist, highly adapted to snowy environments with its wide snowshoe feet and white winter pelage. Besides some

isolated relict populations, it has an impressive, almost continuous distribution across the Palearctic which has persisted through the last ice age (Ferreira et al., 2021; S. Smith et al., 2017). In contrast, the contemporary brown hare populations originate from different refugia in Europe and Near East with temperate, steppe-like climate during the last glacial maximum (Bock, 2020; Fickel et al., 2008). Consequently, typical habitats of the mountain hare, apart for some subspecies, such as the heathland adapted European *L. t. hibernicus* Bell and *L. t. sylvaticus* Nilsson, are circumpolar tundra and taiga (Angerbjorn & Flux, 1995), whereas the brown hare prefers open bushlands and more temperate climate (Bock, 2020; Ognev, 1940). In fact, in Northern Europe, the brown hare has benefitted from land clearance for agriculture as well as shortening of the snow-covered season due to climate change (Levanen, Kunnasranta, & Pohjoismaki, 2018; Thulin, 2003).

Besides the lack of snowshoes and white winter pelage, brown hares are generally 10–20 % larger than mountain hares, reach sexual maturity earlier and have higher reproductive capacity, but shorter lifespan (Angerbjorn & Flux, 1995; Bock, 2020; de Magalhaes, Costa, & Toussaint, 2005; Ernest, 2003; Purvis & Harvey, 1995), characters associated with different life history tactics and trade-offs (Southwood, 1988). Both species are mainly nocturnal, but activity varies depending on the season and weather (Angerbjorn & Flux, 1995; Bock, 2020; Ognev, 1940). Neither species is social or territorial and they do not engage in contest competition, with the exception of males during breeding season (Angerbjorn & Flux, 1995; Bock, 2020). It should be noted that both the mountain hare and brown hare are split to several geographically defined subspecies, which differ in a number physiological characters (Angerbjorn & Flux, 1995; Bock, 2020), but only the nominal subspecies are present in Finland and compared here.

Mountain hare and brown hare have followed radically different evolutionary paths, with multiple selective pressures driving the evolution of the observed morphological, physiological and behavioral differences (Fickel et al., 2008; Reid, 2011; Zimova et al., 2020). While some of these differences are obvious, such as the color of the winter pelage, whose evolution can be understood using modern genomic approaches (Ferreira et al., 2020; Ferreira et al., 2017; Giska et al., 2019; Jones et al., 2018), almost nothing is known about the species differences in the most fundamental cellular housekeeping functions. Housekeeping functions of the cells include the basic gene regulation and expression, maintenance of cellular homeostasis and steady-state metabolism (Eisenberg & Levanon, 2013). Different life history tactics related to metabolism, growth, reproductive capacity and lifespan would be expected to manifest in some of the very basic functions of somatic cells. For instance, arctic hares and snowshoe hares are typically showing a depressed basal metabolic rate during the winter season, which is not present in more temperate species (Sheriff, Kuchel, Boutin, & Humphries, 2009).

It is generally assumed that cellular housekeeping functions are conserved across closely related taxa due to their fundamental importance for the normal function of the organism. Understanding the cellular level species differences not only helps to identify elusive physiological adaptations, but also could shed light on components of the species barrier. The incompatibility in housekeeping functions might contribute to the hybrid disadvantage (Abbott et al., 2013; Arnegard et al., 2014; Burton & Barreto, 2012; Wolf et al., 2010) and reinforce the species separation. This is especially interesting for hares, as despite the recurrent gene flow between many species (Ferreira et al., 2021; Jones et al., 2018; Levanen, Thulin, et al., 2018; Marques, Farelo, et al., 2017; Melo-Ferreira, Boursot, Suchentrunk, Ferrand, & Alves, 2005; Melo-Ferreira, Seixas, et al., 2014; Pohjoismaki et al., 2021) no hybrid species from the ~32 species of genus *Lepus* have been described (A. T. Smith, Johnston, Alves, & Häcklander,

149 2018), unlike in the case of European bison (Soubrier et al., 2016) or clymene dolphin (Amaral,
150 Lovewell, Coelho, Amato, & Rosenbaum, 2014).
151
152 Somatic cells derived from wild animals can be useful models for ecological studies as they
153 may reveal differential susceptibilities of species to toxic pollutants present in their natural
154 habitat (Chen et al., 2009). Fish Gill Cell culture systems, for example, are used for
155 environmental monitoring of water pollution (Wlodkowic & Karpinski, 2021). Cell lines can
156 also inform about zoonotic diseases (Kapczynski, Sweeney, Spackman, Pantin-Jackwood, &
157 Suarez, 2022) or host-parasite interactions (Cano et al., 2019), reducing the need for animal
158 experimentation. Likewise, cell lines ared used to study the nature and evolution of infectious
159 cancers, for example, in dogs (Murgia, Pritchard, Kim, Fassati, & Weiss, 2006) and Tasmanian
160 devils ((Murchison et al., 2010; Pye et al., 2016), offering potential for population screening,
161 drug testing and rescue of endangered species (Belov, 2012; Espejo et al., 2021; Patchett, Flies,
162 Lyons, & Woods, 2020).
163
164 One of the most common cell types used as *in vitro* model are fibroblasts. Fibroblasts originate
165 mainly from mesenchymal cells and are found almost in all tissues of the body. They can also
166 emerge through transition processes from epithelial, endothelial, or adipocyte cells, e.g. after
167 exposure to stress or in pathological conditions (LeBleu & Neilson, 2020). Dermal fibroblasts
168 comprise upper-level (i.e., papillary fibroblasts) and lower-level fibroblast (i.e., reticular
169 fibroblasts), which differ with respect to their morphology, gene expression pattern,
170 proliferation capacity, amount of extracellular matrix production, participation in wound
171 healing processes, secretion of growth factors and immunomodulatory properties (Driskell &
172 Watt, 2015; Janson, Saintigny, van Adrichem, Mahe, & El Ghalbzouri, 2012; Stunova &
173 Vistejnova, 2018). Despite their heterogeneity, dermal fibroblasts have been successfully

174 employed to draw a parallel with the animal physiology (Madelaire, Klink, Israelsen, & Hindle,
175 2022), and several studies have shown positive correlation between resistance to stressors in
176 fibroblasts and a species' life span (Alper, Bronikowski, & Harper, 2015).
177
178 In the present study, we have performed a detailed analysis of fibroblasts isolated from a
179 sympatric population of brown hares and mountain hares, including global gene expression,
180 cell growth and migration, cell cycle control, mitochondrial mass, and oxidative metabolism.
181 We discovered the existence of a species-specific expression of 1,623 genes, which manifested
182 among others in differences in cell cycle control, mitochondrial membrane potential and
183 metabolism. Our results demonstrate that species-specific differences are evident at the level
184 of single cells, including some fundamental housekeeping functions of cells, which could be
185 related to differing life history tactics. Although the physiological traits of cultured fibroblasts
186 are limited compared to the whole organism, cell models offer many interesting and ethically
187 sustainable opportunities to conduct research on wild animals.
188

189 # Materials and methods

190
191 All sample metadata, sequence data as well as final transcriptome data are available through
192 Dryad and SRA depositories (see data accessibility and benefit sharing). Detailed experimental
193 materials and procedures are presented in the Supporting Information Document.
194

Sampling

Four mountain hares (LT 1, 4, 5, 6) and four brown hares (LE 1, 2, 3, 4) were collected by hunting from seven different locations in central parts of southern Finland (Fig. 1A, Table 1). All animals were in reproductive age; sex, collecting date and locality are indicated in Table 1.

Generation of immortalized fibroblast cell lines

One population of immortalized fibroblasts cells was generated from the abdominal skin of each of the eight specimens. The skin biopsies from each animal were separately handled. Each biopsy was cut into smaller pieces and incubated on cell culture plates in standard culture condition. Cells outgrowing the explants were immortalized by large T-antigen transformation and subsampled six times to eliminate non-immortalized cells who undergo senescence. Stocks of immortalized fibroblasts from each animal were cryopreserved in aliquots. The population of immortalized fibroblast from one animal will be referred as a cell line.

RNA isolation and sequencing

For each of the eight hare cell lines, one aliquot of cryopreserved cells was grown in standard cell culture conditions and passaged once onto a 10 cm plate. Upon 80 % confluence, cells were lysed and Poly(A)+ mRNA was isolated. The purified mRNA was sent to the Institute for Molecular Medicine Finland (FIMM) for library preparation and sequencing.

De novo transcriptome assembly

Sequencing adapters and low quality base pairs were trimmed and removed *in silico*. The trimming of the reads was confirmed and inspected before further analysis. *De novo* transcriptome assemblies were created for each species using the Puhti server of the Center for Scientific computing Finland (CSC). For each species, the reads from the four cell lines were

combined to increase the diversity of the final transcriptome assembly. Then assembly was performed.

Validation and transcriptome filtering

To validate the *de novo* transcriptome assemblies, the trimmed reads used to assemble the transcriptome were mapped back on to their respective assembly. To ensure data quality, lowly expressed genes (Li & Dewey, 2011), misassembled transcripts and incomplete transcripts were removed (Smith-Unna, Boursnell, Patro, Hibberd, & Kelly, 2016), and transcripts sharing ≥ 95 % similarity were clustered together (Fu, Niu, Zhu, Wu, & Li, 2012). Completeness of the transcriptomes was then assessed by identifying and comparing single copy orthologs from the transcriptomes against the general and lineage specific databases (Waterhouse et al., 2018).

Functional annotation of transcriptomes

Open reading frames with a minimum length of 200 amino acids were identified *in silico* (Bryant et al., 2017). Transcripts, predicted proteins and protein structure information were retreaved from the SwissProt database (Finn, Clements, & Eddy, 2011) (Petersen, Brunak, von Heijne, & Nielsen, 2011) (Krogh, Larsson, von Heijne, & Sonnhammer, 2001). rRNA genes were separately identified (Lagesen et al., 2007). For each species, the output from each analysis was compiled in the Trinotate SQlite database.

Variant calling of RNAseq data

To infer the genotypes of each cell line, we identified genetic variants by mapping the RNAseq data for each cell line onto Genbank: GCA_009760805.1 pseudo-reference genome (Marques et al., 2020) (Dobin et al., 2013). Variants were then called (Brouard, Schenkel, Marete, & Bissonnette, 2019) and filtered (Danecek et al., 2011) to remove indels, missing data, and hits

with an MAF < 0.05. As of note, as the cell lines are not clonal (i.e. originate from a single founder cell) but from a mixture of cells that grew out of the original explant tissue, *de novo* mutations obtained during the cell culture are rare and excluded from the analysis. Similarly, it is unlikely that a *de novo* mutation increased in frequency due to drift during the limited passage numbers used in this work. Longitudinal studies in more rapidly growing cancer cells have demonstrated that cells maintain a uniform phenotype up to 65 passages (Briske-Anderson, Finley, & Newman, 1997). The resulting VCF file contained one biallelic site for each contig and was analyzed for basic population genomic parameters (Kamvar, Tabima, & Grunwald, 2014). The ancestry coefficient of each cell line was estimated (Frichot & Francois, 2015).

DNA isolation, sexing, mtDNA genotyping and DNA copy number analysis

Total DNA was extracted from each cell line using the peqGOLD Blood and tissue DNA mini kit (VWR Life Science). The sex and mitochondrial DNA (mtDNA) haplotype for each cell line was confirmed by PCR-RFLP of the *ZFX* + *ZFY* loci (Fontanesi et al., 2008; Levänen, Pohjoismäki, & Kunnasranta, 2019) and *CYTB* gene region (Alves, Ferrand, Suchentrunk, & Harris, 2003; Melo-Ferreira et al., 2005), respectively. Mitochondrial DNA copy number was measured with quantitative Real-Time PCR (qPCR) using TaqMan™ chemistry. Primers and TaqMan™ probes (Metabion International AG, Panegg, Germany) were designed to be fully compatible for both species. See Supporting Information Document for primer and probe sequences.

Differential gene expression

As most allelic variants from the two species were initially identified as different genes by the annotation algorithms, defining a common gene set between the two species was essential. To

do this we identified one-to-one reciprocal best BLAST hits following the protocol described by the James Hutton Institute (https://widdowquinn.github.io/2018-03-06-ibioic/02-sequence_databases/05-blast_for_rbh.html). Firstly, the final transcriptome of *L. timidus* was compared against the final transcriptome of the *L. europaeus*. Then the reciprocal BLAST analysis was performed by comparing the transcriptome of L. *europaeus* to the *L. timidus* transcriptome. Transcripts identified as reciprocal best BLAST hits as determined by the bit score were then extracted from the final transcriptomes into species-specific fasta files. The trimmed reads for all samples were then mapped onto the one-to-one reciprocal best BLAST hits of *L. timidus* and then *L. europaeus* using bowtie2 version 2.4.4 with the following parameters --all --min-score L,-0.1,-0.1. The resulting alignment files were then clustered and quantified using Corset version 1.09 (Davidson & Oshlack, 2014) to minimize the effect of gene isoforms in the differential expression. The raw count table was analyzed for differentially expressed genes with DESeq2(Love, Huber, & Anders, 2014), using the Integrative Differential Expression Analysis for Multiple Experiments (IDEAMEX) webtool (Jimenez-Jacinto, Sanchez-Flores, & Vega-Alvarado, 2019). DESeq2 internally calculates the geometric mean of each gene and then normalizes the raw gene count by dividing the gene count by this mean. Visualization of the RNAseq analysis results was then performed in R using ggplot2 (Ginestet, 2011), to produce PCA plots, heatmaps and volcano plots.

Cell growth measurements

Nuclei counting

For each of the eight cell lines, one aliquot of cryopreserved cells was grown in standard culture conditions and passaged once. From each line, the passaged cells were resuspended and seeded into 48-well plates at low density. Every 24 hours, cells from four wells per cell line were fixed

and stained with Hoechst fluorescent nuclear marker. For each well, the nuclei present in four non-overlapping images were counted. For each cell line, growth was obtained as the slope of the $ln(count) = f(t)$ curves and used for statistical analysis (16 measurements per cell line). Growth was converted to cell doubling times (CDT) for graphical presentation.

Cell counting

For each of the eight cell lines, one aliquot of cryopreserved cells was grown in standard culture conditions and passaged once. The passaged cells were resuspended, and a subpopulation was seeded at low density in one well of a 12-well plate, each of the 8 cell lines being represented in the same plate. After 24 hours, the plate was transferred to a cell imaging system adjusted to the standard culture conditions. Twelve non-overlapping phase contrast images were captured per well (i.e., per cell line) every 24 hours over a period of 96 hours. Fibroblasts were manually counted using Fiji-ImageJ. Statistical analysis (12 measures per cell line) and graphic presentation as for nuclei counting. Comparison of the cell counting vs. nuclei counting is presented in S-Figs. 1–4 (see Supplementary methods for further information).

Cell cycle measurements

For each of the eight cell lines, one aliquot of cryopreserved cells was grown in standard culture conditions and passaged once. A subpopulation from each plate was distributed into 6-well plates, 3 wells per time point and two wells for controls. The cells were grown until 80 % density before treatment. For each cell line and timepoint, the treatment was performed in three and omitted in two (untreated control) of the wells. Treatment consisted in exposure to aphidicolin, a reversible inhibitor of the nuclear replicative DNA polymerase, which arrests the cell cycle at the G1 to S transition. At timepoint 0, the cells from five of the wells per cell line (three treated and two untreated wells) were transferred to collection tubes for analysis. All

other cells were kept in the plate, but washed and exposed to media without aphidicolin, allowing synchronized restart of the cell cycle in the treated samples. Every three hours, cells from three wells per cell line (only treated) were collected. RNA was eliminated and nuclei were stained with propidium iodine (PI), a fluorescent DNA-intercalating dye. PI staining intensity was measured for each sample by flow cytometry of the cell population. The numbers of cells in G1, S, and G2 phase were analyzed using CytExpert software. Statistical analyses were performed only for the treated cells (three measures per cell line per timepoint), on each phase of the cycle separately, using the untreated cells as a reference to distinguish the phases and control for the cell cycle blockage.

Wound healing assays

Wound healing assays were performed essentially as in (Jonkman et al., 2014). For each of the eight cell lines, one aliquot of cryopreserved cells was grown in standard culture conditions and passaged. A subpopulation from each cell line was distributed into two 12-well plate, each line being represented once per plate. Cells were grown until forming a continuous monolayer. Manual scratching was performed with a sterile micropipette tip in each well. Cells were rinsed and maintained in standard culture conditions in the microscope stage of either an EVOS® FL (plate 1) or a Cell-IQ® (plate 2) instrument. For each well, phase contrast images of the wound were captured every hour from three non-overlapping areas for 48 hours. Wound healing was derived in Fiji-ImageJ using MRI Wound Healing tool (Volker Baecker, Montpellier RIO Imaging, Montpellier, France) from the linear migration phase and converted into wound closure rate ($WCR = \frac{|slope|}{2*l}$). In addition, the lag-time before the start of linear migration phase ($T_{0\text{-linear}} - T_0$) was estimated. Separate statistical analyses were performed on the wound closure rate and on the lag time (12 measures per cell line).

Mitochondrial mass measurements

For each of the eight cell lines, one aliquot of cryopreserved cells was grown in standard culture conditions and passaged. A subpopulation of each cell line was then grown in a cell culture plate until 80 % confluent. Cells from each line were then suspended and divided in seven aliquots. Three aliquots were stained with nonylacridine orange (NAO), a cell-permeant fluorescent marker of the mitochondrial mass. In three other aliquots mitochondria were uncoupled with FCCP prior to NAO staining. The last unstained aliquot served as a negative control. Intensity of NAO staining was measured by flow cytometry. Analysis was performed with FlowJo™ software (Version 10.7.2. Ashland, OR: Becton, Dickinson and Company; 2021). Separate statistical analyses were performed on the samples treated with NAO and on the samples treated with NAO and on those treated with NAO + FCCP (6 measures per cell line, in both cases).

Mitochondrial membrane potential measurement

Cells were obtained as described for the mitochondrial mass measurements, except that the cells from each line were divided in three aliquots. Staining was performed in the presence of Verapamil, which blocks a membrane transporter interfering with the staining (Morganti, Bonora, Ito, & Ito, 2019). To estimate mitochondrial membrane potential, fibroblasts were exposed to a cell-permeant fluorescent dye, tetramethylrhodamine (TMRM). The intensity of TMRM staining was measured by flow cytometry. The results were analysed using FlowJo software. Positive and negative controls were obtained respectively treating cells with the FCCP uncoupler and blocking H^+ re-entry with Oligomycin before staining. Corrected TMRM intensities ($TMRM - TMRM_{FCCP}$) were used as response variable for the statistical analysis (12 measures per cell line).

Mitochondrial morphology

Cells were obtained as described for the previous procedures except that cells from each line were seeded on glass bottom poly-d-lysine-coated plates and grown until reaching 70 % confluence. Before imaging, the medium was refreshed and cells were stained with MitoTracker Deep Red FM plus NucBlue dyes. Cells were rinsed with 1× PBS and maintained in 1× PBS during imaging by Olympus IX70 Inverted Fluorescence Microscope. Images were processed in Fiji-ImageJ software.

Mitochondrial respiration measurements

Cells were obtained as described for previous procedure except that cells from each line were grown on 10 cm^2 plates until 80 % confluence. Media was refreshed one hour prior to cell collection. For each measurement, 5×10^6 cells were suspended in respiration buffer and immediately transferred into the chamber of a respirometer. Two chambers were used, allowing to simultaneously analyse one LE and one LT sample. Oxygen consumption was analysed after digitonin permeabilization of the cells by sequential addition of substrates and inhibitors as described in Fig. 3D and supplementary material. For each cell line, four independent measurements were performed. Respirometry data were analysed with two-way ANOVA (Genotype × Compound) with interactions. It is important to note that very small differences in respirometry (as observed here) are very near to the instrument's measurement error.

Protein preparation and Western blotting

Cells grown to 80 % confluence were collected, washed with ice-cold DPBS and lysed in ice-cold RIPA buffer supplemented with Protease Inhibitors. Insoluble material was eliminated by centrifugation before storing the protein extracts at -80 °C. Protein concentration was measured by BCA assay (Pierce, #23225). 30 µg protein per sample was loaded in one well of a precast

gel (Biorad, #5678093). Spectra Multicolor Broad Range (Thermo Scientific™, #26634) was used as a molecular size ladder. Electrophoresis was performed at 100 V for 80 min before transferring the proteins onto nitrocellulose membranes (Biorad, #1704158, #1704159). Blots were washed, blocked and probed with beta-Actin, COXIV, SDHA, TOM20, VDAC1 or Vinculin primary antibody. After over-night incubation at 4 ^{o}C, blots were washed and exposed to a peroxidase-labelled secondary antibody for 2 hours. Blots were washed and visualized using a horseradish peroxidase assay. Images were obtained with ChemiDoc XRS^{+} Imaging System (Biorad, #1708265), quantified in Image Lab software and normalised to the reference proteins (beta-Actin or Vinculin). Separate statistical analyses (three measures per cell line) were performed on each of normalized protein levels (COX IV, SDHA, TOM2 and VDAC1).

Statistical analysis

Statical analysis was performed in R using glm and gamlss modelling (Rigby & Stasinopoulos, 2005). The response variable is indicated in the specific method section. The predictor of interest was the species, the cell line being nested into it (for cell cycle analyses species:time was also a predictor of interest). For each response variable, all the relevant gamlss distributions were fitted onto the nested model, ranked by AICc and curated based on the quality of the residuals. The importance of each predictor and interaction was assessed by ANOVA analysis of the best distribution compatible with glm modeling. Significance and intensity of the effect(s) of interest are reported in the results sections and figure legends. Note that this approach verified the between-species differences found with simpler tests (two-way ANOVA, T-test & Mann-Whitney), which are therefore not presented.

Results

Genotype and ancestry validation of the hare cell lines

All eight cell lines (LE for *Lepus europaeus* or brown hare and LT for *Lepus timidus* or mountain hare) originate from sympatric hare populations across southern Finland (Fig. 1A, Table 1). As mountain hares frequently hybridize with brown hares, producing fertile hybrids and therefore forming potential hybrid continuums in the populations of both species, we first wanted to confirm the genotypes and the ancestry of the cell lines. For the nuclear DNA genotyping, we used 9,056 SNPs in 519,066–549,582 transcripts obtained from the RNAseq data (Fig. 1B, S-Tables 1–2), while the mitochondrial DNA (mtDNA) identity and sex of the cell lines was checked using PCR-RFLP.

The cell lines of the two species formed distinct and species-specific clusters in the PCA analysis of the SNP differences; the brown hare samples clustered notably tight compared to the mountain hares (Fig. 1B). This difference can be attributed to the low levels of heterozygosity in brown hares compared to the mountain hare samples (Fig. 1C). The clustering of the samples also did not correlate with the geographic origin of the animals, giving confidence that the cell lines represent independent and unrelated biological replicates. In ancestry coefficient analysis each cell line fit uniformly under the assigned species with no or minimal evidence of ancestral hybridization (Fig. 1D). The cell lines showing evidence of low level mixed ancestry were the mountain hare cell lines LT5 (~3 %) and LT6 (~1 %) as well as brown hare cell line LE3 (~1 %). All cell lines had conspecific mtDNA, and the male to female ratio was 3:1 in mountain hares and 1:1 in brown hares (Table 1).

Differential gene expression between species

We next looked at the global gene expression differences between the cell lines. When all 400,000+ transcripts i.e., including all allelic variants and isoforms that were different enough to be counted as separate genes by the algorithm, were compared (S-Table 2), mountain hare and brown hare cell lines formed species-specific clusters (Fig. 1E–F). Remarkably, the intraspecific variance in mRNA expression levels was similar in both species (Fig. 1F) and did not correlate with the genotypic variability (Fig. 1B). The species-specific expression pattern was considerably weaker when the 16,689 orthologous genes were compared (S-Table 2, Fig. 1E). According to this analysis, the gene expression of brown hare cell line LE1 more resembled that of the mountain hare cells. One-to-one reciprocal BLAST, used to find ortholog genes, showed the average sequence divergence between the transcripts from the two species to be 1.08 % (range 0–28 %).

As much of the observed total transcriptome differences could be attributed to species-specific isoforms and allelic variants, more detailed differential expression analyses were performed only with the orthologues (S-Table 2). Gene ontology (GO)-term analysis of the expression of the orthologous genes revealed 1,623 differentially expressed genes associated with various GO-terms. Over a hundred different genetic processes or cellular components showed a significant ($p < 0.001$) difference between the two species (S-Table 3, for full DE table per orthologous transcript see S-Table 4). The most notable difference between the two species was that brown hares showed higher expression of genes involved in basic housekeeping functions of cells, such as oxidative energy metabolism, cell migration and cell cycle regulation (Fig. 2A). For example, several genes related to mitochondrial function (*PDK4*, *FMC1*, *ATPK*, *ACADL* and *PPARG*) had higher expression levels in brown hares (Fig. 2B). In contrast, many genes showing higher expression in mountain hare were orphan or master regulators of cell

functions, such as the L-xylulose reductase enzyme (*DCXR*), the transcriptional inactivator *PAGR1* (Zhang, Sun, Cho, Chow, & Simons, 2013), the regulator of cell fate, proliferation and differentiation *NOTC3* (Choy et al., 2017), as well as the high-fat diet associated hormonal regulator *ENHO* (Jasaszwili, Billert, Strowski, Nowak, & Skrzypski, 2020).

Cell proliferation is faster in brown hares

Fibroblasts maintain the organism's structure by producing and maintaining an extracellular matrix (ECM), a network of connective proteins that hold tissues and organs in place. As such, they are efficiently attaching and growing on non-coated polystyrene surfaces. Changes in fibroblasts ability to proliferate or synthesize ECM should translate in measurable growth changes. Adaptation to long chronic exposure to cold is a factor that distinguishes mountain hare and brown hare evolutionary histories. This has been shown to redirect energy use towards maintenance of cellular function and organism, with consequences like delay in growth and sexual maturity in a large range of models (Nussey, Froy, Lemaitre, Gaillard, & Austad, 2013). We therefore postulated that mountain hare cell lines would grow slower than the brown hare ones. When cultured on non-coated polystyrene surfaces, the brown hare cells showed significantly faster cell doubling time (Fig. 4A) compared to mountain hares. Maintaining cells in low glucose medium, which generally promotes oxidative metabolism over glycolysis, did not influence the overall species difference (Fig. 4A). There were also notable cell-line differences within the species (S-Figs. 1–4).

Wound healing is faster in brown hares

Fibroblasts are also very important for wound healing. During this process, their role is to regenerate the scaffold onto which the new skin will be built (Driskell & Watt, 2015; Janson et al., 2012; Stunova & Vistejnova, 2018). Fibroblasts participate in this phenomenon by

proliferating, but also by migrating and modifying their shape and volume. Due to the role of wound healing in organism maintenance, we expected that advantages in migration and cell motility might balance the slower proliferation in mountain hare. We tested this hypothesis by scraping a ~600 μm wide gap in a continuous layer of fibroblasts cells (see methods section). Similar to our observations of cell proliferation, wound closure was slower in mountain hare compared to brown hare cells (Fig. 4B). Curiously though, mountain hare fibroblasts showed a smaller delay in the initiation of the wound closure (Fig. 4B). Like with the cell growth, within species differences in wound healing were smaller than the between species difference (S-Figs. 5–6).

Differences in cell proliferation and migration can be attributed to cell cycle differences

While GO-term analysis can identify differences in gene expression patterns, it seldomly reveals insights about their phenotypic consequences. In our analysis two observations seem to go hand in hand: brown hare fibroblasts proliferate faster (Fig. 4A) and they express higher levels of genes related to cell cycle (Fig. 2A). As immortalized fibroblasts should proliferate at near maximum capacity in cell culture conditions, we wanted to understand the biological reason behind the species difference in more detail. The cell cycle consists of the primary growth phase G1, where cells grow in size. Once the cells are large enough, they enter S-phase, where the nuclear DNA is duplicated, which is followed by the G2- or secondary growth-phase preceding mitosis (M-phase). By synchronizing the cells, we were able to show that while there was no difference in the G1-phase between the two species, mountain hare cells pass faster through the S-phase than the brown hare cells, but stay systematically longer in the G2/M-phase (Fig. 5). This difference was not explained by the size of the cytoplasm required to grow

514 before the mitosis, as all cells were relatively variable in size and shape, regardless of the
515 species (Fig. 6, S-Fig. 7).
516
517 **Mountain and brown hare fibroblast mitochondria have similar energetic capacity**
518 The enrichment of mitochondria-related gene expression in brown hare cells is interesting, as
519 enhanced oxidative metabolism might reflect a general physiological difference in energy
520 expenditure and utilization between the species. Oxidative metabolism can be directly assessed
521 through respirometry where mitochondria are exposed to respiratory chain substates, and their
522 oxygen consumption is measured. Unexpectedly, we did not observe significant differences in
523 mitochondrial mass (Fig. 3A, S-Figs. 8–9), cell respiration (Fig. 3C–D), mtDNA copy number
524 (Fig. 3E) or selected mitochondrial protein levels (Fig. 3E, S-Fig. 10), except for COX4 protein
525 levels, which were lower in LT fibroblasts.
526
527 **Mountain hare fibroblast mitochondria have higher mitochondrial membrane**
528 **potential**
529 The mitochondrial membrane potential (MMP) is the difference in charge across the inner
530 mitochondrial membrane (IMM). It is increased when the respiratory chain uses the energy
531 from catabolic reactions to pump H^+ across the IMM. It is consumed when the ATP synthase
532 transfers the H^+ back into the matrix to generate ATP. MMP is known to influence reduction-
533 oxidation balance, Ca^{2+} and AMPK signaling (Chandel, 2015), but also histone acetylation
534 (Martinez-Reyes & Chandel, 2020), oxidative stress and apoptosis (Zorova et al., 2018).
535 Because MMP is very dynamic and sensitive to genetic as well as environmental conditions, it
536 was difficult to predict how mountain and brown hare fibroblasts would differ. To assess MMP
537 we used TMRM, a non-toxic cell-permeant potentiometric fluorescent dye which accumulates
538 into mitochondria based on the MMP and can be measured by flow cytometry (see methods).

Mountain hare fibroblasts showed dramatically higher accumulation of TMRM (Fig. 3B), indicating a higher MMP in mountain hares compared to brown hares. Within species differences among the cell lines were also observed (S-Fig. 11).

Discussion

Species differences can manifest as phenotypic adaptations to different ecological niches, accompanied by discrete morphological features, which are often obvious for the observer and also form the basis for taxonomic species separation. However, very little is known about differences in the fundamental cellular functions among closely related species. This is not only important in understanding the molecular mechanisms behind observable phenotypic differences, but also serves as notice to studies generalizing findings from one species (typically human, mouse or another model organism) across a wider spectrum of biodiversity. Furthermore, as we will discuss, differences in life history tactics are likely to manifest also at the cellular level.

Our focus has been on comparing mountain hare and brown hare, which form a very interesting species pair to study. While the two species live in sympatry at the northern edges of the brown hare range, they are very different in their morphology and ecology. As pointed out earlier, the two species hybridize, producing fertile offspring, resulting in gene flow across the species barrier (Alves et al., 2003; Fredsted, Wincentz, & Villesen, 2006; Jansson, Thulin, & Pehrson, 2007; Levanen, Kunnasranta, et al., 2018; Levänen et al., 2019; Levanen, Thulin, et al., 2018; Melo-Ferreira et al., 2005; Pohjoismaki et al., 2021; Reid, 2011; Thulin, 2003; Thulin, Stone, Tegelström, & Walker, 2006; Thulin & Tegelström, 2002). However, the two species have not merged and despite the relative commonness of first generation hybrids, the proportion of hybrid ancestry in Nordic hare populations is small (Fredsted et al., 2006; Jansson & Pehrson, 2007; Jansson et al., 2007; Levanen, Kunnasranta, et al., 2018; Levänen et al., 2019; Levanen,

Thulin, et al., 2018; Pohjoismaki et al., 2021; Thulin, 2003; Thulin, Jaarola, & Tegelström, 1997; Thulin et al., 2006; Thulin & Tegelström, 2002). It is plausible that significant differences in basic house-keeping functions of cells could contribute to the hybrid incompatibility and maintenance of the species barrier.

Fibroblasts as a model for testing species difference

Cell lines cannot recapitulate the physiology and metabolism of the entire animal, however, fundamental phenotypic features in cells should have consequences also at the organismal level. In the presented study, our primary interest was to investigate if cell lines from two closely related and interbreeding species of hares would show differences in their cellular functions. By applying some of the common methods in cell biology for the phenotypic analysis of these non-model organisms, we were able to verify the existence of these differences. For example, our results show that fibroblasts from mountain hares perform slower in growth and wound healing experiments than those of brown hares.

Based on our findings we conclude that the usage of cell lines is legitimate as a preliminary or even a substitute to study for the physiology of wild animals. However, establishing cell lines require careful consideration. Firstly, many cell types, including fibroblasts, have distinct embryonic origins (Driskell & Watt, 2015), leading to epigenetic, gene regulatory and consequently physiological differences. Therefore, fibroblasts should always be collected from the same anatomical region and their origin should be verified through genetic analysis. Secondly, all somatic cells acquire mutations and eventually enter senescence, therefore care should be taken to collect samples of reasonable size (> 10000 progenitor cells), from ~ age matched individuals, to minimize cell culture duration and variations, and to immortalize the cells. Transformation with the large T-antigen of SV40 virus is usually preferred, as it preserve

most of the cell's original features (Kirchhoff et al., 2004), including species-specific differences. T-antigen leads to the inactivation of p53 and pRB tumor suppressor genes and causes genetic instability in some cells, leading to their demise, while simultaneously givin grise to a subpopulation of surviving cells with indefinite growth capacity and preserved genome integrity. Hence, immortalized cell lines can be regarded as mixed populations due to (1) the number of progenitors, which might each harbour different random mutations and (2) the genetic consequence of the immortalization process. Importantly, mutations are subject to selection by growth competition in cell culture, which leads to the convergence of phenotypic properties. Therefore, due to the selective convergence caused by the cell isolation, immortalization and culture, the observed differences between the fibroblasts from the two hare species are likely to robustly represent true, although conservative species differences.

It should be noted that also the comparison of the transcriptomes of two species is not trivial: the genetic differences between the two species cluttered the gene annotation pipeline, as evident from the large number of detected genes in the first pass of the data analysis (Table 3). We therefore developed an alternative approach to compare only the orthologous genes. This provided a more robust set of common genes to compare, although it likely missed interesting genes expressed in a strict species-specific manner. It is also noteworthy that the number of orthologous genes found by reciprocal BLAST search differed from the polypeptide-encoding gene count based on the predicted ORFs. This is due to the fact that some truncated transcript sequences do not contain ORFs, while others might be present only in one species.

While many of the features showed variability between the cell lines, including cell morphology (Fig. 6, S-Fig. 7), the species separation existed also when the samples were clustered based on the levels of orthologous transcripts (Fig. 1G). This is important as several

subtypes of dermal fibroblasts are known from mammals (Jiang & Rinkevich, 2018), which could have influenced the analysis. However, any cell line deviating from the others would have been visible as an outlier in the analysis due to the cell type-specific gene expression patterns. If one imagines that the separation of the cell lines along the first component axis would represent different cell types, these form a continuum along this axis (Fig. 1G). This is not compatible with the idea of having discrete fibroblast subtypes with typical expression patterns (Buechler et al., 2021), but would fit well with individual differences between the specimens. Furthermore, it is likely that the used isolation method, as pointed out above, sampling sections of the skin as well as the culture conditions favor some fibroblast types over others.

Genetic diversity *vs.* phenotypic diversity among Finnish hares

Although the sampled animals come from a geographic region where the two hare species live in sympatry (Fig. 1A, Table 1), none of the cell lines showed notable hybrid ancestry based on the global transcript sequence genotypes (Fig. 1B, D). The genotyping also confirmed previous observations finding much lower genetic diversity in the Finnish brown hares than in the mountain hares (Fig. 1B, C). Low genetic diversity is typical for expanding populations due to the founder effect and genetic drift at the expansion front (Chuang & Peterson, 2016). We have shown previously that brown hares obtain genetic variation from mountain hares through hybridization (Levanen, Thulin, et al., 2018; Pohjoismaki et al., 2021). This is also evidenced in the present data (Fig. 1B), when comparing the low number of private alleles (878) in brown hares and the number of alleles shared between the species (2,130) with the high number of private alleles (6,048) in the mountain hare. While some of these alleles probably represent true trans-species polymorphisms, predating the species split, the disproportionate number of shared alleles in brown hares is better explained by frequent hybridization with mountain hare

639 at the expansion front, which steadily decreases when the brown hare population gets
640 established (Levanen, Thulin, et al., 2018). The phenotypic effects of the introgression are still
641 unclear.
642
643 While the sample set of eight cell lines is small for a population genetic analysis, the lack of
644 genetic structure among the specimens is remarkable. For example, the mountain hare sample
645 LT1 from Ilomantsi, representing a typical boreal taiga forest location, is very similar to the
646 LT4 specimen from Vesilahti, some 420 km apart and representing mostly agricultural
647 landscapes dominated by brown hares (Table 1, Fig. 1A, B, D). Interestingly, none of the brown
648 hare cell lines from Eastern Finland showed noticeable ancestral hybridization with mountain
649 hare (Fig. 1D), although hybridization is relatively common in this region due to the large
650 mountain hare populations (Levanen, Kunnasranta, et al., 2018). However, this might be
651 caused by the analysis being performed with coding sequence variation, therefore violating the
652 assumption of neutrality underlying such population genetic analyses. In this case, it might be
653 that differential selection pressures are maintaining the species difference, inviting future
654 studies to compare coding vs. non-coding variation in sympatric populations of the two species.
655
656 Although the brown hare cells showed little genetic diversity compared to the mountain hares
657 (Fig. 1B), the two species showed similar variability at the level of gene expression (Fig. 1F,
658 G). While it is plausible that the brown hares retain more genetic variation in the control regions
659 of genes, it is unlikely that there would be no correlation between non-coding and coding
660 variation in the hare genomes. The results are likely to reflect the fact that gene expression is
661 influenced by several intrinsic as well as environmental factors, giving it a good degree of
662 variation even under controlled cell culture conditions. As the RNA was isolated from non-
663 synchronized cells with similar confluence, fluctuations caused by cell-cell interaction should

664 have averaged out. In contrast, cell cycle-dependent gene expression may underlie some of the
665 species' differences, as mountain hare cells spend more time G2, but less in S phase (Fig. 5).
666
667 **Adaptations or noise – molecular constituents of a species difference?**
668 Perhaps the most notable difference between the two species was the faster proliferation and
669 migration rates of the brown hare cells compared to mountain hare (Fig. 4). This difference
670 was also evident from the fact that brown hare cells showed higher expression of genes related
671 to mitotic cell cycle and cell migration (Fig. 2A), indicating that these cells divide more
672 frequently or exit the cell cycle less frequently than mountain hare cells. Analysis of
673 synchronized cell populations showed that mountain hare cells progress through the S phase
674 faster than brown hare ones but take longer to complete the G2 phase (Fig. 5). The faster
675 progression through the S phase could be related to the shorter lag time for mountain hares in
676 the wound healing assay, although a considerably longer G2 phase makes the overall process
677 slower (Fig. 4B). Generally, faster S phase suggests faster DNA replication and/or repair,
678 whereas slower G2 could mean that mountain hare cells need more time than brown hares to
679 build up cytoplasm, cell organelles or storages for the mitosis. From the adaptational
680 perspective, this could reflect differences in biosynthetic capacity or cell cycle quality controls.
681
682 One of the differentially regulated cellular components picked up in the transcriptome analysis
683 were mitochondria (Fig. 2). We found this potentially interesting, as energy expenditure and
684 its fine tuning by mitochondrial metabolism might show correspondence with the requirements
685 of environmental adaptation between arctic vs. temperate species, as well as be related to the
686 basic metabolic rate of the animal. However, we found no correlation with mitochondria-
687 related gene expression, mitochondrial mass, cell respiration or mtDNA copy number, and little
688 correlation with the levels of various mitochondrial proteins (only one out of four

mitochondrial genes studied, Fig. 3). Still, the slightly higher respiration in *L. europaeus* cell lines (albeit not significant) could be related to the higher COX4 (subunit of respiratory complex IV) protein level and would deserve further studies, maybe using different respiratory substrates (e.g., fatty acids). However, one mitochondrial parameter was showing a major species difference, namely the mitochondrial membrane potential (MMP), which was higher in mountain hare cells (Fig. 3B). To our knowledge, this is the first report of a species difference in MMP. MMP corresponds to the difference in overall charge between the mitochondrial matrix and the intermembrane space (also known as $\Delta\Psi m$) (Zorova et al., 2018). The inner mitochondrial membrane is impermeable to nearly all molecules including H^+. As the inner mitochondrial membrane hosts the respiratory chain, which pumps H^+ from the matrix to the intermembrane space, the MMP gradient increases. However, the inner mitochondrial membrane also includes ATP synthase, which transfers H^+ back into mitochondria to produce ATP, and thereby decreasing the MMP gradient. Therefore, the MMP is a dynamic marker of mitochondrial energetics. Physiologically high MMP indicates a positive energetic balance (production > demand), whereas pathologically high MMP is associated with increased ROS production and eventually apoptosis or necrosis. Physiologically low MMP is a sign of energy depletion (production < demand). Low MMP due to e.g. respiratory chain dysfunction can cause mitochondrial fragmentation and elimination or repair of mitochondria with low MMP, but also apoptosis. Differences in MMP may therefore reflect cell-level difference in metabolism and may have consequences in cellular stress adaptation. These two possibilities are now under scrutiny.

It is noteworthy that the organization and function of the OXPHOS system, which is constrained by co-evolution of mitochondrial and nuclear genomes, is very conserved in animals (Burton & Barreto, 2012; Tobler, Barts, & Greenway, 2019) and therefore likely to

714 evolve slowly in aerobic animals. However, features such as the mitochondrial membrane
715 potential are controlled at multiple levels and can be seen as a signature of the cellular
716 metabolism. As the environmental factors are tightly controlled in cell culture conditions, it
717 should be possible to identify the genetic changes associated with the species differences in the
718 MMP. Sequence comparison for a subset of mitochondria-related proteins, using e.g.,
719 MitoCarta as reference (Rath et al., 2021) may reveal potentially interesting gene candidates.
720 However, the differences might be related to the different glycolytic or other general metabolic
721 activities, which may be under the control of regulatory mechanisms that evolved differently
722 in the two species. We believe that a global metabolic analysis of the fibroblasts of these two
723 hare species may help narrowing down the candidate genes and their functional differences
724 between the two species. This could lead to a better understanding of the adaptive evolution of
725 metabolic traits and their role in speciation.
726
727 Mitochondria play a key role also in the adaptation to chronic exposure to low temperatures,
728 which is another critical factor that distinguishes the mountain hare and brown hare
729 evolutionary history. In animals, adaptation to cold involves behavioral (sheltering &
730 migration), organismal and cellular adaptation. At the organismal level, adaptation through
731 improved insulation is often observed; decreasing exposure of body surface by adapting a
732 specific coating (winter fur) and increasing skin thickness (subcutaneous white adipose tissue
733 in humans) are two major mechanisms. Having very little subcutaneous white adipose tissue,
734 hares rely on fur and thermogenesis (Ikeda et al., 2017) to maintain body temperature. As no
735 enzymatic reaction is 100 % efficient, increase in basal cellular metabolism and decrease in
736 metabolic efficiencies will directly translate into increased thermogenesis. Increased metabolic
737 wasting in mountain hares could therefore be a part of a cold adaptive trade-off. Constitutive
738 wasting in basal metabolic reactions would translate in less efficient specialized functions, such

739 as growth and wound healing in mountain hare. We are presently testing the differences of
740 thermogenesis in these fibroblasts.
741
742 In general, cellular adaptation to cold occurs through inducible response, mediated by muscle
743 (shivering) and adipose tissue (OXPHOS-dependent thermogenesis). In brown and beige
744 adipocytes, upon induction of cold resistance, the proton gradient causing the membrane
745 potential is diminished by the mitochondrial uncoupling protein 1 (UCP1), leading to all the
746 energy being dissipated as heat (Chouchani, Kazak, & Spiegelman, 2019; Cioffi et al., 2009;
747 Nowack, Giroud, Arnold, & Ruf, 2017). A higher mitochondrial membrane potential in
748 mountain hares would mean also a higher potential for heat generation by uncoupling (Fig.
749 3B). The observation that the mountain hare-specific *UCP1* alleles are under positive selection
750 in Finnish brown hares (Pohjoismaki et al., 2021), warrants for comparison of the uncoupling
751 efficiency of hare alleles in the future. Fibroblasts do not express UCP1, but can differentiate
752 to beige adipocytes having UCP1.
753
754 Altogether, the observed cellular differences suggest differential partitioning of resources
755 within the cells, which could recapitulate the differences in the life history strategies of the two
756 species (Promislow & Harvey, 1990). For example, it is plausible that the slower cell
757 proliferation and migration rate, faster S phase and slower G2 phase, coupled with higher MMP
758 are a signature of a greater allocation of resources towards maintenance of cells at the expense
759 of growth and basal metabolism in mountain hare. For a given organism, delaying the age of
760 reproduction would require a larger investment of resource in somatic maintenance. If energy
761 sources are limited, this is traded for a slower development (Kirkwood, 1977). Interestingly,
762 mountain hares have a longer lifespan, lower fertility, longer gestation time, smaller litter size
763 and delayed reproductive maturity compared to brown hares (Angerbjorn & Flux, 1995; Bock,

2020; de Magalhaes et al., 2005; Ernest, 2003; Ognev, 1940; Purvis & Harvey, 1995). Interestingly, these same features are under positive selection in populations exposed to caloric restriction, in parallel with lowering of the animals' metabolic rate (Gibbs & Reynolds, 2012; Nussey et al., 2013). Our observations could therefore highlight the most elementary manifestation of this investment difference into pace of living.

Using cultured cells for wild animal research and future of the field

Cultured cells isolated from animals are often believed to be poorly fit for population studies and to have limited value in terms of physiological representativity, compared to whole animal or *ex vivo* tissue samples. However, they can offer interesting opportunities to address questions in the field of ecology and evolutionary biology. Firstly, they allow the study of rare or endangered animals using small biopsies (e.g. ear-punch) from anesthetized animals (Madelaire et al., 2022).

Secondly, immortalized cells can be preserved frozen for almost indefinite time and expanded to large scale at any time, providing a nearly infinite source of RNA and DNA. In fact, the RNA-sequencing data provided with this paper represents the most comprehensive transcriptome data profiling of mountain hares (Marques, Ferreira, et al., 2017; Marques et al., 2020) and brown hare (Amoutzias et al., 2016).

Thirdly, methods in cell and molecular biology provide exciting opportunities to experimentally test genotype to phenotype association even in extinct species. For example, transfected cells were used to identify coat color polymorphism in woolly mammoths caused by an amino acid substitution in the *Mc1r* gene (Rompler et al., 2006). In addition, cell cultures can be used to investigate the comparative physiology of aging between long-living species,

such as microbats and birds, and “traditional” short-living models, like rodents and fruit flies (Harper & Holmes, 2021). It should be also possible to narrow down candidate genes behind many cell traits and critically test their influence on the trait using CRISPR-Cas9 knockout and/or transgenic expression of alternative allelic variants.

Finally, fibroblasts are known to have a strong degree of de-differentiation potential (LeBleu & Neilson, 2020), making them a prime candidate for establishment of induced pluripotent stem cells (iPSCs), which can then be maintained indefinitely, but also differentiated in any cell type (Malik & Rao, 2013). iPSCs can even be used for assisted reproduction (Selvaraj, Wildt, & Pukazhenthi, 2011). For this reason significant efforts have been made to obtain fibroblast-derived iPSCs from vulnerable and endangered species (Ben-Nun et al., 2011) (Ramaswamy et al., 2015), (Weeratunga et al., 2020) (Verma et al., 2013). Successful generation of iPSCs from skin derived fibroblasts has been described in rabbits (Gavin-Plagne et al., 2020), but the method has not been validated for hares.

In conclusion, the differences between two closely related hare species clearly manifested as phenotypic differences in a cell model, which are likely to reflect biologically meaningful, adaptive features of the animals. Understanding the molecular mechanisms behind these cellular differences will help to shed light on the constituents of species boundaries, genetic basis of adaptation and genotype to phenotype correlations.

Acknowledgements

We would like to thank Mr Lauri Peippo (Parikkala, Finland), Mr Jukka Pusa (Joensuu, Finland) and Mr Jari Kokkonen (Kontiolahti, Finland) for providing the samples for LT6, LE1

and LE3, respectively. This study belongs to the xHARES consortium funded by the R'Life initiative of the Academy of Finland, grant number 329264.

This research paper is dedicated to the home country of the first author, Ukraine, and all people who stand to protect world peace, democracy, and freedom.

References

Abbott, R., Albach, D., Ansell, S., Arntzen, J. W., Baird, S. J., Bierne, N., . . . Zinner, D. (2013). Hybridization and speciation. *J Evol Biol, 26*(2), 229-246. doi:10.1111/j.1420-9101.2012.02599.x

Adavoudi, R., & Pilot, M. (2021). Consequences of Hybridization in Mammals: A Systematic Review. *Genes (Basel), 13*(1). doi:10.3390/genes13010050

Alper, S. J., Bronikowski, A. M., & Harper, J. M. (2015). Comparative cellular biogerontology: Where do we stand? *Exp Gerontol, 71*, 109-117. doi:10.1016/j.exger.2015.08.018

Alves, P. C., Ferrand, N., Suchentrunk, F., & Harris, D. J. (2003). Ancient introgression of Lepus timidus mtDNA into L-granatensis and L-europaeus in the Iberian Peninsula. *Molecular Phylogenetics and Evolution, 27*(1), 70-80. doi:10.1016/S1055-7903(02)00417-7

Alves, P. C., Melo-Ferreira, J., Freitas, H., & Boursot, P. (2008). The ubiquitous mountain hare mitochondria: multiple introgressive hybridization in hares, genus Lepus. *Philosophical Transactions of the Royal Society B-Biological Sciences, 363*(1505), 2831-2839. doi:10.1098/rstb.2008.0053

Amaral, A. R., Lovewell, G., Coelho, M. M., Amato, G., & Rosenbaum, H. C. (2014). Hybrid speciation in a marine mammal: the clymene dolphin (Stenella clymene). *Plos One, 9*(1), e83645. doi:10.1371/journal.pone.0083645

Amoutzias, G. D., Giannoulis, T., Moutou, K. A., Psarra, A. M., Stamatis, C., Tsipourlianos, A., & Mamuris, Z. (2016). SNP Identification through Transcriptome Analysis of the European Brown Hare (Lepus europaeus): Cellular Energetics and Mother's Curse. *Plos One, 11*(7), e0159939. doi:10.1371/journal.pone.0159939

Angerbjorn, A., & Flux, J. E. C. (1995). Lepus timidus. *Mammalian Species, 495*, 1-11.

Arnegard, M. E., McGee, M. D., Matthews, B., Marchinko, K. B., Conte, G. L., Kabir, S., . . . Schluter, D. (2014). Genetics of ecological divergence during speciation. *Nature, 511*(7509), 307-311. doi:10.1038/nature13301

Belov, K. (2012). Contagious cancer: lessons from the devil and the dog. *Bioessays, 34*(4), 285-292. doi:10.1002/bies.201100161

Ben-Nun, I. F., Montague, S. C., Houck, M. L., Tran, H. T., Garitaonandia, I., Leonardo, T. R., . . . Loring, J. F. (2011). Induced pluripotent stem cells from highly endangered species. *Nat Methods, 8*(10), 829-831. doi:10.1038/nmeth.1706

Bock, A. (2020). Lepus europaeus (Lagomorpha: Leporidae). *Mammalian Species, 52*(997), 125-142. doi:https://doi.org/10.1093/mspecies/seaa010

Briske-Anderson, M. J., Finley, J. W., & Newman, S. M. (1997). The influence of culture time and passage number on the morphological and physiological development of Caco-2 cells. *Proc Soc Exp Biol Med, 214*(3), 248-257. doi:10.3181/00379727-214-44093

Brouard, J. S., Schenkel, F., Marete, A., & Bissonnette, N. (2019). The GATK joint genotyping workflow is appropriate for calling variants in RNA-seq experiments. *J Anim Sci Biotechnol, 10*, 44. doi:10.1186/s40104-019-0359-0

Bryant, D. M., Johnson, K., DiTommaso, T., Tickle, T., Couger, M. B., Payzin-Dogru, D., . . . Whited, J. L. (2017). A Tissue-Mapped Axolotl De Novo Transcriptome Enables Identification of Limb Regeneration Factors. *Cell Reports, 18*(3), 762-776. doi:10.1016/j.celrep.2016.12.063

Buechler, M. B., Pradhan, R. N., Krishnamurty, A. T., Cox, C., Calviello, A. K., Wang, A. W., . . . Turley, S. J. (2021). Cross-tissue organization of the fibroblast lineage. *Nature, 593*(7860), 575-579. doi:10.1038/s41586-021-03549-5

Burton, R. S., & Barreto, F. S. (2012). A disproportionate role for mtDNA in Dobzhansky-Muller incompatibilities? *Mol Ecol, 21*(20), 4942-4957. doi:10.1111/mec.12006

Burton, R. S., Ellison, C. K., & Harrison, J. S. (2006). The sorry state of F2 hybrids: consequences of rapid mitochondrial DNA evolution in allopatric populations. *Am Nat, 168 Suppl 6*, S14-24. doi:10.1086/509046

Cano, I., Taylor, N. G., Bayley, A., Gunning, S., McCullough, R., Bateman, K., . . . Paley, R. K. (2019). In vitro gill cell monolayer successfully reproduces in vivo Atlantic salmon host responses to Neoparamoeba perurans infection. *Fish Shellfish Immunol, 86*, 287-300. doi:10.1016/j.fsi.2018.11.029

Chan, K. M. A., & Levin, S. A. (2005). Leaky prezygotic isolation and porous genomes: Rapid introgression of maternally inherited DNA. *Evolution, 59*(4), 720-729.

Chandel, N. S. (2015). Evolution of Mitochondria as Signaling Organelles. *Cell Metab, 22*(2), 204-206. doi:10.1016/j.cmet.2015.05.013

Chen, T. L., Wise, S. S., Kraus, S., Shaffiey, F., Levine, K. M., Thompson, W. D., . . . Wise, J. P. (2009). Particulate Hexavalent Chromium is Cytotoxic and Genotoxic to the North Atlantic Right Whale (Eubalaena glacialis) Lung and Skin Fibroblasts. *Environmental and Molecular Mutagenesis, 50*(5), 387-393. doi:10.1002/em.20471

Chouchani, E. T., Kazak, L., & Spiegelman, B. M. (2019). New Advances in Adaptive Thermogenesis: UCP1 and Beyond. *Cell Metab, 29*(1), 27-37. doi:10.1016/j.cmet.2018.11.002

Choy, L., Hagenbeek, T. J., Solon, M., French, D., Finkle, D., Shelton, A., . . . Siebel, C. W. (2017). Constitutive NOTCH3 Signaling Promotes the Growth of Basal Breast Cancers. *Cancer Res, 77*(6), 1439-1452. doi:10.1158/0008-5472.CAN-16-1022

Chuang, A., & Peterson, C. R. (2016). Expanding population edges: theories, traits, and trade-offs. *Global Change Biology, 22*(2), 494-512. doi:10.1111/gcb.13107

Cioffi, F., Senese, R., de Lange, P., Goglia, F., Lanni, A., & Lombardi, A. (2009). Uncoupling proteins: a complex journey to function discovery. *Biofactors, 35*(5), 417-428. doi:10.1002/biof.54

Danecek, P., Auton, A., Abecasis, G., Albers, C. A., Banks, E., DePristo, M. A., . . . Genomes Project Analysis, G. (2011). The variant call format and VCFtools. *Bioinformatics, 27*(15), 2156-2158. doi:10.1093/bioinformatics/btr330

Davidson, N. M., & Oshlack, A. (2014). Corset: enabling differential gene expression analysis for de novo assembled transcriptomes. *Genome Biol, 15*(7), 410. doi:10.1186/s13059-014-0410-6

de Magalhaes, J. P., Costa, J., & Toussaint, O. (2005). HAGR: the Human Ageing Genomic Resources. *Nucleic Acids Res, 33*(Database issue), D537-543. doi:10.1093/nar/gki017

Dobin, A., Davis, C. A., Schlesinger, F., Drenkow, J., Zaleski, C., Jha, S., . . . Gingeras, T. R. (2013). STAR: ultrafast universal RNA-seq aligner. *Bioinformatics, 29*(1), 15-21. doi:10.1093/bioinformatics/bts635

Dobzhansky, T. (1937). *Genetics and the Origin of Species*. New York: Columbia University Press.
Driskell, R. R., & Watt, F. M. (2015). Understanding fibroblast heterogeneity in the skin. *Trends Cell Biol, 25*(2), 92-99. doi:10.1016/j.tcb.2014.10.001
Eisenberg, E., & Levanon, E. Y. (2013). Human housekeeping genes, revisited. *Trends Genet, 29*(10), 569-574. doi:10.1016/j.tig.2013.05.010
Ernest, S. K. M. (2003). Life history characteristics of placental non-volant mammals. *Ecology, 84*, 3402-3402.
Espejo, C., Wilson, R., Willms, E., Ruiz-Aravena, M., Pye, R. J., Jones, M. E., . . . Lyons, A. B. (2021). Extracellular vesicle proteomes of two transmissible cancers of Tasmanian devils reveal tenascin-C as a serum-based differential diagnostic biomarker. *Cell Mol Life Sci, 78*(23), 7537-7555. doi:10.1007/s00018-021-03955-y
Ferreira, M. S., Alves, P. C., Callahan, C. M., Giska, I., Farelo, L., Jenny, H., . . . Melo-Ferreira, J. (2020). Transcriptomic regulation of seasonal coat color change in hares. *Ecol Evol, 10*(3), 1180-1192. doi:10.1002/ece3.5956
Ferreira, M. S., Alves, P. C., Callahan, C. M., Marques, J. P., Mills, L. S., Good, J. M., & Melo-Ferreira, J. (2017). The transcriptional landscape of seasonal coat colour moult in the snowshoe hare. *Mol Ecol, 26*(16), 4173-4185. doi:10.1111/mec.14177
Ferreira, M. S., Jones, M. R., Callahan, C. M., Farelo, L., Tolesa, Z., Suchentrunk, F., . . . Melo-Ferreira, J. (2021). The Legacy of Recurrent Introgression during the Radiation of Hares. *Syst Biol, 70*(3), 593-607. doi:10.1093/sysbio/syaa088
Fickel, J., Hauffe, H. C., Pecchioli, E., Soriguer, R., Vapa, L., & Pitra, C. (2008). Cladogenesis of the European brown hare (Lepus europaeus Pallas, 1778). *European Journal of Wildlife Research, 54*(3), 495-510. doi:10.1007/s10344-008-0175-x
Finn, R. D., Clements, J., & Eddy, S. R. (2011). HMMER web server: interactive sequence similarity searching. *Nucleic Acids Res, 39*(Web Server issue), W29-37. doi:10.1093/nar/gkr367
Fontanesi, L., Tazzoli, M., Pecchioli, E., Hauffe, H. C., Robinson, T. J., & Russo, V. (2008). Sexing European rabbits (Oryctolagus cuniculus), European brown hares (Lepus europaeus) and mountain hares (Lepus timidus) with ZFX and ZFY loci. *Mol Ecol Resour, 8*(6), 1294-1296. doi:10.1111/j.1755-0998.2008.02167.x
Fredsted, T., Wincentz, T., & Villesen, P. (2006). Introgression of mountain hare (Lepus timidus) mitochondrial DNA into wild brown hares (Lepus europaeus) in Denmark. *BMC Ecol, 6*, 17. doi:10.1186/1472-6785-6-17
Frichot, E., & Francois, O. (2015). LEA: An R package for landscape and ecological association studies. *Methods in Ecology and Evolution, 6*(8), 925-929. doi:10.1111/2041-210x.12382
Fu, L., Niu, B., Zhu, Z., Wu, S., & Li, W. (2012). CD-HIT: accelerated for clustering the next-generation sequencing data. *Bioinformatics, 28*(23), 3150-3152. doi:10.1093/bioinformatics/bts565
Gavin-Plagne, L., Perold, F., Osteil, P., Voisin, S., Moreira, S. C., Combourieu, Q., . . . Afanassieff, M. (2020). Insights into Species Preservation: Cryobanking of Rabbit Somatic and Pluripotent Stem Cells. *Int J Mol Sci, 21*(19). doi:10.3390/ijms21197285
Gibbs, A. G., & Reynolds, L. A. (2012). *Drosophila as a Model for Starvation: Evolution, Physiology, and Genetics.* Heidelberg, Germany: Springer.
Ginestet, C. (2011). ggplot2: Elegant Graphics for Data Analysis. *Journal of the Royal Statistical Society Series a-Statistics in Society, 174*, 245-245. doi:DOI 10.1111/j.1467-985X.2010.00676_9.x
Giska, I., Farelo, L., Pimenta, J., Seixas, F. A., Ferreira, M. S., Marques, J. P., . . . Melo-Ferreira, J. (2019). Introgression drives repeated evolution of winter coat color

polymorphism in hares. *Proc Natl Acad Sci U S A, 116*(48), 24150-24156. doi:10.1073/pnas.1910471116

Hamilton, J. A., & Miller, J. M. (2016). Adaptive introgression as a resource for management and genetic conservation in a changing climate. *Conservation Biology, 30*(1), 33-41. doi:10.1111/cobi.12574

Harper, J. M., & Holmes, D. J. (2021). New Perspectives on Avian Models for Studies of Basic Aging Processes. *Biomedicines, 9*(6). doi:10.3390/biomedicines9060649

Harrison, R. G., & Larson, E. L. (2014). Hybridization, introgression, and the nature of species boundaries. *J Hered, 105 Suppl 1*, 795-809. doi:10.1093/jhered/esu033

Hedrick, P. W. (2013). Adaptive introgression in animals: examples and comparison to new mutation and standing variation as sources of adaptive variation. *Mol Ecol, 22*(18), 4606-4618. doi:10.1111/mec.12415

Ikeda, K., Kang, Q., Yoneshiro, T., Camporez, J. P., Maki, H., Homma, M., . . . Kajimura, S. (2017). UCP1-independent signaling involving SERCA2b-mediated calcium cycling regulates beige fat thermogenesis and systemic glucose homeostasis. *Nat Med, 23*(12), 1454-1465. doi:10.1038/nm.4429

Janson, D. G., Saintigny, G., van Adrichem, A., Mahe, C., & El Ghalbzouri, A. (2012). Different gene expression patterns in human papillary and reticular fibroblasts. *J Invest Dermatol, 132*(11), 2565-2572. doi:10.1038/jid.2012.192

Jansson, G., & Pehrson, A. (2007). The recent expansion of the brown hare (Lepus europaeus) in Sweden with possible implications to the mountain hare (L. timidus). *European Journal of Wildlife Research, 53*(2), 125-130. doi:10.1007/s10344-007-0086-2

Jansson, G., Thulin, C.-G., & Pehrson, A. (2007). Factors related to the occurrence of hybrids between brown hares Lepus europaeus and mountain hares L-timidus in Sweden. *Ecography, 30*(5), 709-715. doi:10.1111/j.2007.0906-7590.05162.x

Jasaszwili, M., Billert, M., Strowski, M. Z., Nowak, K. W., & Skrzypski, M. (2020). Adropin as A Fat-Burning Hormone with Multiple Functions-Review of a Decade of Research. *Molecules, 25*(3). doi:10.3390/molecules25030549

Jhuang, H. Y., Lee, H. Y., & Leu, J. Y. (2017). Mitochondrial-nuclear co-evolution leads to hybrid incompatibility through pentatricopeptide repeat proteins. *EMBO Rep, 18*(1), 87-101. doi:10.15252/embr.201643311

Jiang, D., & Rinkevich, Y. (2018). Defining Skin Fibroblastic Cell Types Beyond CD90. *Front Cell Dev Biol, 6*, 133. doi:10.3389/fcell.2018.00133

Jimenez-Jacinto, V., Sanchez-Flores, A., & Vega-Alvarado, L. (2019). Integrative Differential Expression Analysis for Multiple EXperiments (IDEAMEX): A Web Server Tool for Integrated RNA-Seq Data Analysis. *Front Genet, 10*, 279. doi:10.3389/fgene.2019.00279

Jones, M. R., Mills, L. S., Alves, P. C., Callahan, C. M., Alves, J. M., Lafferty, D. J. R., . . . Good, J. M. (2018). Adaptive introgression underlies polymorphic seasonal camouflage in snowshoe hares. *Science, 360*(6395), 1355-1358. doi:10.1126/science.aar5273

Jonkman, J. E., Cathcart, J. A., Xu, F., Bartolini, M. E., Amon, J. E., Stevens, K. M., & Colarusso, P. (2014). An introduction to the wound healing assay using live-cell microscopy. *Cell Adh Migr, 8*(5), 440-451. doi:10.4161/cam.36224

Kamvar, Z. N., Tabima, J. F., & Grunwald, N. J. (2014). Poppr: an R package for genetic analysis of populations with clonal, partially clonal, and/or sexual reproduction. *PeerJ, 2*, e281. doi:10.7717/peerj.281

Kapczynski, D. R., Sweeney, R., Spackman, E., Pantin-Jackwood, M., & Suarez, D. L. (2022). Development of an in vitro model for animal species susceptibility to SARS-CoV-2 replication based on expression of ACE2 and TMPRSS2 in avian cells. *Virology, 569*, 1-12. doi:10.1016/j.virol.2022.01.014

1003 Kirchhoff, C., Araki, Y., Huhtaniemi, I., Matusik, R. J., Osterhoff, C., Poutanen, M., . . .
1004 Orgebin-Crist, M. C. (2004). Immortalization by large T-antigen of the adult
1005 epididymal duct epithelium. *Mol Cell Endocrinol, 216*(1-2), 83-94.
1006 doi:10.1016/j.mce.2003.10.073
1007 Kirkwood, T. B. (1977). Evolution of ageing. *Nature, 270*(5635), 301-304.
1008 doi:10.1038/270301a0
1009 Krogh, A., Larsson, B., von Heijne, G., & Sonnhammer, E. L. (2001). Predicting
1010 transmembrane protein topology with a hidden Markov model: application to complete
1011 genomes. *J Mol Biol, 305*(3), 567-580. doi:10.1006/jmbi.2000.4315
1012 Lagesen, K., Hallin, P., Rodland, E. A., Staerfeldt, H. H., Rognes, T., & Ussery, D. W. (2007).
1013 RNAmmer: consistent and rapid annotation of ribosomal RNA genes. *Nucleic Acids*
1014 *Res, 35*(9), 3100-3108. doi:10.1093/nar/gkm160
1015 LeBleu, V. S., & Neilson, E. G. (2020). Origin and functional heterogeneity of fibroblasts.
1016 *FASEB J, 34*(3), 3519-3536. doi:10.1096/fj.201903188R
1017 Levanen, R., Kunnasranta, M., & Pohjoismaki, J. (2018). Mitochondrial DNA introgression at
1018 the northern edge of the brown hare (Lepus europaeus) range. *Annales Zoologici*
1019 *Fennici, 55*(1-3), 15-24.
1020 Levänen, R., Pohjoismäki, J., & Kunnasranta, M. (2019). Home ranges of semi-urban brown
1021 hares (Lepus europaeus) and mountain hares (Lepus timidus) at northern latitudes.
1022 *Annales Zoologici Fennici, 56*, 107–120.
1023 Levanen, R., Thulin, C. G., Spong, G., & Pohjoismaki, J. L. O. (2018). Widespread
1024 introgression of mountain hare genes into Fennoscandian brown hare populations. *Plos*
1025 *One, 13*(1). doi:ARTN e0191790
1026 10.1371/journal.pone.0191790
1027 Li, B., & Dewey, C. N. (2011). RSEM: accurate transcript quantification from RNA-Seq data
1028 with or without a reference genome. *Bmc Bioinformatics, 12*. doi:Artn 323
1029 10.1186/1471-2105-12-323
1030 Love, M. I., Huber, W., & Anders, S. (2014). Moderated estimation of fold change and
1031 dispersion for RNA-seq data with DESeq2. *Genome Biol, 15*(12), 550.
1032 doi:10.1186/s13059-014-0550-8
1033 MacColl, A. D. (2011). The ecological causes of evolution. *Trends Ecol Evol, 26*(10), 514-522.
1034 doi:10.1016/j.tree.2011.06.009
1035 Madelaire, C. B., Klink, A. C., Israelsen, W. J., & Hindle, A. G. (2022). Fibroblasts as an
1036 experimental model system for the study of comparative physiology. *Comp Biochem*
1037 *Physiol B Biochem Mol Biol, 260*, 110735. doi:10.1016/j.cbpb.2022.110735
1038 Malik, N., & Rao, M. S. (2013). A review of the methods for human iPSC derivation. *Methods*
1039 *Mol Biol, 997*, 23-33. doi:10.1007/978-1-62703-348-0_3
1040 Mallet, J., Besansky, N., & Hahn, M. W. (2016). How reticulated are species? *Bioessays, 38*(2),
1041 140-149. doi:10.1002/bies.201500149
1042 Marques, J. P., Farelo, L., Vilela, J., Vanderpool, D., Alves, P. C., Good, J. M., . . . Melo-
1043 Ferreira, J. (2017). Range expansion underlies historical introgressive hybridization in
1044 the Iberian hare. *Scientific Reports, 7*. doi:Artn 40788
1045 10.1038/Srep40788
1046 Marques, J. P., Ferreira, M. S., Farelo, L., Callahan, C. M., Hacklander, K., Jenny, H., . . .
1047 Melo-Ferreira, J. (2017). Mountain hare transcriptome and diagnostic markers as
1048 resources to monitor hybridization with European hares. *Sci Data, 4*, 170178.
1049 doi:10.1038/sdata.2017.178
1050 Marques, J. P., Seixas, F. A., Farelo, L., Callahan, C. M., Good, J. M., Montgomery, W. I., . .
1051 . Melo-Ferreira, J. (2020). An Annotated Draft Genome of the Mountain Hare (Lepus
1052 timidus). *Genome Biology and Evolution, 12*(1), 3656-3662. doi:10.1093/gbe/evz273

1053 Martinez-Reyes, I., & Chandel, N. S. (2020). Mitochondrial TCA cycle metabolites control
1054 physiology and disease. *Nat Commun, 11*(1), 102. doi:10.1038/s41467-019-13668-3
1055 Mayr, E. (1942). *Systematics and the origin of species from the viewpoint of a zoologist*. New
1056 York: Columbia University Press.
1057 Melo-Ferreira, J., Boursot, P., Suchentrunk, F., Ferrand, N., & Alves, P. C. (2005). Invasion
1058 from the cold past: extensive introgression of mountain hare (Lepus timidus)
1059 mitochondrial DNA into three other hare species in northern Iberia. *Mol Ecol, 14*(8),
1060 2459-2464. doi:10.1111/j.1365-294X.2005.02599.x
1061 Melo-Ferreira, J., Farelo, L., Freitas, H., Suchentrunk, F., Boursot, P., & Alves, P. C. (2014).
1062 Home-loving boreal hare mitochondria survived several invasions in Iberia: the relative
1063 roles of recurrent hybridisation and allele surfing. *Heredity, 112*(3), 265-273.
1064 doi:10.1038/hdy.2013.102
1065 Melo-Ferreira, J., Seixas, F. A., Cheng, E., Mills, L. S., & Alves, P. C. (2014). The hidden
1066 history of the snowshoe hare, Lepus americanus: extensive mitochondrial DNA
1067 introgression inferred from multilocus genetic variation. *Mol Ecol, 23*(18), 4617-4630.
1068 doi:10.1111/mec.12886
1069 Morganti, C., Bonora, M., Ito, K., & Ito, K. (2019). Electron transport chain complex II sustains
1070 high mitochondrial membrane potential in hematopoietic stem and progenitor cells.
1071 *Stem Cell Res, 40*, 101573. doi:10.1016/j.scr.2019.101573
1072 Murchison, E. P., Tovar, C., Hsu, A., Bender, H. S., Kheradpour, P., Rebbeck, C. A., . . .
1073 Papenfuss, A. T. (2010). The Tasmanian devil transcriptome reveals Schwann cell
1074 origins of a clonally transmissible cancer. *Science, 327*(5961), 84-87.
1075 doi:10.1126/science.1180616
1076 Murgia, C., Pritchard, J. K., Kim, S. Y., Fassati, A., & Weiss, R. A. (2006). Clonal origin and
1077 evolution of a transmissible cancer. *Cell, 126*(3), 477-487.
1078 doi:10.1016/j.cell.2006.05.051
1079 Nowack, J., Giroud, S., Arnold, W., & Ruf, T. (2017). Muscle Non-shivering Thermogenesis
1080 and Its Role in the Evolution of Endothermy. *Front Physiol, 8*, 889.
1081 doi:10.3389/fphys.2017.00889
1082 Nussey, D. H., Froy, H., Lemaitre, J. F., Gaillard, J. M., & Austad, S. N. (2013). Senescence
1083 in natural populations of animals: widespread evidence and its implications for bio-
1084 gerontology. *Ageing Res Rev, 12*(1), 214-225. doi:10.1016/j.arr.2012.07.004
1085 Ognev, S. I. (1940). 157. Lepus (Eulagus) europeaus Pall. (1778) заяц-русак. In *Mammals of*
1086 *the USSR and adjacent countries: rodents (In Russian)* (Vol. 4, pp. 112-161). Moscow:
1087 Akademiya Nauk SSSR.
1088 Patchett, A. L., Flies, A. S., Lyons, A. B., & Woods, G. M. (2020). Curse of the devil: molecular
1089 insights into the emergence of transmissible cancers in the Tasmanian devil
1090 (Sarcophilus harrisii). *Cell Mol Life Sci, 77*(13), 2507-2525. doi:10.1007/s00018-019-
1091 03435-4
1092 Petersen, T. N., Brunak, S., von Heijne, G., & Nielsen, H. (2011). SignalP 4.0: discriminating
1093 signal peptides from transmembrane regions. *Nat Methods, 8*(10), 785-786.
1094 doi:10.1038/nmeth.1701
1095 Pohjoismaki, J. L. O., Michell, C., Levanen, R., & Smith, S. (2021). Hybridization with
1096 mountain hares increases the functional allelic repertoire in brown hares. *Sci Rep, 11*(1),
1097 15771. doi:10.1038/s41598-021-95357-0
1098 Promislow, D. E. L., & Harvey, P. H. (1990). Living fast and dying young: A comparative
1099 analysis of life-history variation among mammals. *Journal of Zoology, 220*, 417–437.
1100 Purvis, A., & Harvey, P. H. (1995). Mammal life-history evolution: a comparative test of
1101 Charnov's model. *Journal of Zoology, 237*, 259-283.

Pye, R. J., Pemberton, D., Tovar, C., Tubio, J. M., Dun, K. A., Fox, S., . . . Woods, G. M. (2016). A second transmissible cancer in Tasmanian devils. *Proc Natl Acad Sci U S A, 113*(2), 374-379. doi:10.1073/pnas.1519691113

Ramaswamy, K., Yik, W. Y., Wang, X. M., Oliphant, E. N., Lu, W., Shibata, D., . . . Hacia, J. G. (2015). Derivation of induced pluripotent stem cells from orangutan skin fibroblasts. *BMC Res Notes, 8*, 577. doi:10.1186/s13104-015-1567-0

Reid, N. (2011). European hare (Lepus europaeus) invasion ecology: implication for the conservation of the endemic Irish hare (Lepus timidus hibernicus). *Biological Invasions, 13*(3), 559-569. doi:10.1007/s10530-010-9849-x

Rigby, R. A., & Stasinopoulos, D. A. (2005). Generalized additive models for location, scale and shape. *Journal of the Royal Statistical Society: Series C (Applied Statistics), 54*, 507-554. doi:https://doi.org/10.1111/j.1467-9876.2005.00510.x

Rompler, H., Rohland, N., Lalueza-Fox, C., Willerslev, E., Kuznetsova, T., Rabeder, G., . . . Hofreiter, M. (2006). Nuclear gene indicates coat-color polymorphism in mammoths. *Science, 313*(5783), 62. doi:10.1126/science.1128994

Schluter, D., & Conte, G. L. (2009). Genetics and ecological speciation. *Proc Natl Acad Sci U S A, 106 Suppl 1*, 9955-9962. doi:10.1073/pnas.0901264106

Selvaraj, V., Wildt, D. E., & Pukazhenthi, B. S. (2011). Induced pluripotent stem cells for conserving endangered species? *Nat Methods, 8*(10), 805-807. doi:10.1038/nmeth.1715

Sheriff, M. J., Kuchel, L., Boutin, S., & Humphries, M. M. (2009). Seasonal Metabolic Acclimatization in a Northern Population of Free-Ranging Snowshoe Hares, Lepus Americanus. *Journal of Mammalogy, 90*(3), 761-767. doi:Doi 10.1644/08-Mamm-a-247r.1

Smith, A. T., Johnston, C. H., Alves, P. C., & Häcklander, K. (2018). *Lagomorphs: pikas, rabbits and hares of the world.* Baltimore: Johns Hopkins University Press.

Smith, S., Sandoval-Castellanos, E., Lagerholm, V. K., Napierala, H., Sablin, M., Von Seth, J., . . . Dalen, L. (2017). Nonreceding hare lines: genetic continuity since the Late Pleistocene in European mountain hares (Lepus timidus). *Biological Journal of the Linnean Society, 120*(4), 891-908.

Smith-Unna, R., Boursnell, C., Patro, R., Hibberd, J. M., & Kelly, S. (2016). TransRate: reference-free quality assessment of de novo transcriptome assemblies. *Genome Res, 26*(8), 1134-1144. doi:10.1101/gr.196469.115

Soubrier, J., Gower, G., Chen, K., Richards, S. M., Llamas, B., Mitchell, K. J., . . . Cooper, A. (2016). Early cave art and ancient DNA record the origin of European bison. *Nat Commun, 7*, 13158. doi:10.1038/ncomms13158

Southwood, T. R. E. (1988). Tactics, strategies and templets. *Oikos, 52*, 3-18.

Stunova, A., & Vistejnova, L. (2018). Dermal fibroblasts-A heterogeneous population with regulatory function in wound healing. *Cytokine Growth Factor Rev, 39*, 137-150. doi:10.1016/j.cytogfr.2018.01.003

Thulin, C.-G. (2003). The distribution of mountain hares (Lepus timidus, L. 1758) in Europe: A challenge from brown hares (L. europaeus, Pall. 1778)? *Mammal Review, 33*(1), 29-42. doi:DOI 10.1046/j.1365-2907.2003.00008.x

Thulin, C.-G., Jaarola, M., & Tegelström, H. (1997). The occurrence of mountain hare mitochondrial DNA in wild brown hares. *Mol Ecol, 6*(5), 463-467.

Thulin, C.-G., Stone, J., Tegelström, H., & Walker, C. W. (2006). Species assignment and hybrid identification among Scandinavian hares Lepus europaeus and L. timidus. *Wildlife Biology, 12*(1), 29-38. doi:Doi 10.2981/0909-6396(2006)12[29:Saahia]2.0.Co;2

Thulin, C.-G., & Tegelström, H. (2002). Biased geographical distribution of mitochondrial DNA that passed the species barrier from mountain hares to brown hares (genus Lepus): an effect of genetic incompatibility and mating behaviour? *Journal of Zoology, 258*, 299-306. doi:10.1017/S0952836902001425

Tobler, M., Barts, N., & Greenway, R. (2019). Mitochondria and the Origin of Species: Bridging Genetic and Ecological Perspectives on Speciation Processes. *Integr Comp Biol, 59*(4), 900-911. doi:10.1093/icb/icz025

Todesco, M., Pascual, M. A., Owens, G. L., Ostevik, K. L., Moyers, B. T., Hubner, S., . . . Rieseberg, L. H. (2016). Hybridization and extinction. *Evolutionary Applications, 9*(7), 892-908. doi:10.1111/eva.12367

Verma, R., Liu, J., Holland, M. K., Temple-Smith, P., Williamson, M., & Verma, P. J. (2013). Nanog is an essential factor for induction of pluripotency in somatic cells from endangered felids. *Biores Open Access, 2*(1), 72-76. doi:10.1089/biores.2012.0297

Waterhouse, R. M., Seppey, M., Simao, F. A., Manni, M., Ioannidis, P., Klioutchnikov, G., . . . Zdobnov, E. M. (2018). BUSCO Applications from Quality Assessments to Gene Prediction and Phylogenomics. *Mol Biol Evol, 35*(3), 543-548. doi:10.1093/molbev/msx319

Weeratunga, P., Shahsavari, A., Fennis, E., Wolvetang, E. J., Ovchinnikov, D. A., & Whitworth, D. J. (2020). Induced Pluripotent Stem Cell-Derived Mesenchymal Stem Cells from the Tasmanian Devil (Sarcophilus harrisii) Express Immunomodulatory Factors and a Tropism Toward Devil Facial Tumor Cells. *Stem Cells Dev, 29*(1), 25-37. doi:10.1089/scd.2019.0203

Wlodkowic, D., & Karpinski, T. M. (2021). Live-Cell Systems in Real-Time Biomonitoring of Water Pollution: Practical Considerations and Future Perspectives. *Sensors (Basel), 21*(21). doi:10.3390/s21217028

Wolf, J. B., Lindell, J., & Backstrom, N. (2010). Speciation genetics: current status and evolving approaches. *Philos Trans R Soc Lond B Biol Sci, 365*(1547), 1717-1733. doi:10.1098/rstb.2010.0023

Zhang, Z., Sun, Y., Cho, Y. W., Chow, C. C., & Simons, S. S., Jr. (2013). PA1 protein, a new competitive decelerator acting at more than one step to impede glucocorticoid receptor-mediated transactivation. *J Biol Chem, 288*(1), 42-58. doi:10.1074/jbc.M112.427740

Zimova, M., Giery, S. T., Newey, S., Nowak, J. J., Spencer, M., & Mills, L. S. (2020). Lack of phenological shift leads to increased camouflage mismatch in mountain hares. *Proc Biol Sci, 287*(1941), 20201786. doi:10.1098/rspb.2020.1786

Zorova, L. D., Popkov, V. A., Plotnikov, E. Y., Silachev, D. N., Pevzner, I. B., Jankauskas, S. S., . . . Zorov, D. B. (2018). Mitochondrial membrane potential. *Anal Biochem, 552*, 50-59. doi:10.1016/j.ab.2017.07.009

Data Accessibility and Benefit-Sharing Statement

Genetic data:

All data are available through the Dryad depository under Gaertner, Kateryna et al. (2022),

Molecular phenotyping uncovers differences in basic housekeeping functions among closely

related species of hares (Lepus spp., Lagomorpha: Leporidae), Dryad, Dataset, https://doi.org/10.5061/dryad.p8cz8w9sm

Raw sequence reads are deposited in the SRA under the accession numbers given in Table 2.

Sample metadata:

Metadata is presented in Table 1 as well as stored in the SRA (see Table 2).

Research material availability:

The authors are willing to share the cell lines, reagents, laboratory notes and advice upon reasonable request for non-commercial purposes.

Benefits Generated:

All collaborators are included as co-authors; the results of research have been shared with the provider communities and the broader scientific community. More broadly, our group is committed to international scientific partnerships, as well as institutional capacity building. The contributions of all individuals to the research, including hunters, are described in the METHODS and ACKNOWLEDGEMENTS. All data have been shared with the broader public via appropriate biological databases.

Author contributions

Designed research: JLOP, ED, KG, CM; Performed research: KG, CM, ED, RT, SG, SES, JP; Contributed new reagents or analytical tools: CM, SG, MS; Analyzed data: KG, CM, ED, RT, JP; Wrote the paper: JP, ED, KG, CM, SG.

Tables

Table 1. Species, locality data, sex and mtDNA haplotype of the cell lines used in the study. All individuals were adults.

Species	Cell line ID	Collection locality	Longitude;Latitude	Sampling date	Sex	mtDNA
Lepus timidus	LT1	Ilomantsi	63.0609;30.6248	September 2018	Male	*timidus*
	LT4	Vesilahti	61.2671;23.4845	January 2020	Female	*timidus*
	LT5	Outokumpu	62.7595;28.9765	January 2020	Male	*timidus*
	LT6	Ruokolahti	61.3390;28.8804	February 2020	Male	*timidus*
Lepus europaeus	LE1	Liperi	62.6207;29.4478	October 2019	Male	*europaeus*
	LE2	Outokumpu	62.6212;29.0733	November 2019	Female	*europaeus*
	LE3	Kontiolahti	62.6508;29.7507	January 2020	Female	*europaeus*
	LE4	Vesilahti	61.2937;23.4590	January 2020	Male	*europaeus*

1216

1217 Table 2. RNA sequencing read counts and SRA accession numbers for the cell lines.

Species	Cell line ID	Raw reads (PE)	Trimmed reads (PE)	SRA accession number
Lepus timidus	LT1	121,730,308	112,751,292	SAMN27555144
	LT4	124,677,084	116,762,368	SAMN27555145
	LT5	81,927,034	75,606,128	SAMN27555146
	LT6	183,597,094	171,314,838	SAMN27555147
Lepus europaeus	LE1	269,577,848	250,703,284	SAMN27555148
	LE2	141,499,210	130,128,674	SAMN27555149
	LE3	188,717,244	174,701,744	SAMN27555150
	LE4	197,190,242	178,804,524	SAMN27555151

1218

1219 Table 3. Transcriptome statistics for the cell lines. The number of genes corresponds to unique
1220 transcripts and includes all allelic variants. Transdecoder was used to find genes based on
1221 complete ORFs and does not include truncated sequences, which contribute to the orthologue
1222 gene count.

		Species	
		Lepus europaeus	*Lepus timidus*
Raw	Number of Genes	419,721	413,402

	Number of Transcripts	549,582	519,066
	Total assembled bases	499,766,067	445,061,170
	Contig N50	2,020	1,918
	Contig N50 - longest isoforms only	716	658
	GC content (%)	49.8	49.55
Highly expressed - longest isoform only	Retained (% of input retained)	419,721 (76.37)	413,402 (79.64)
	Contig N50	622	583
	GC content	47.93	47.71
CD-Hit-EST 95%	Retained (% of input retained)	408,827 (97.40)	404,443 (97.83)
	Contig N50	631	589
	GC content (%)	47.9	47.69
High quality contigs	Retained (% of input retained)	398,741 (97.53)	395,469 (97.78)
	Contig N50	639	596
	GC content (%)	47.89	47.67
Transdecoder "-m 200 amino acids" *	Number of ORFs	16,879	16,071
Reciprocal BLAST (orthologue count)	Number of 1:1 reciprocal BLAST hits	16,689	16,689

Figures

Fig. 1. Overview of the sample distribution, genotypes and transcriptomes of the hare cell lines. (A) Geographic location of the hare specimens collected for the study. (B) PCA plot of the sample genotypes based on 9,056 SNPs in 519,066–549,582 transcripts. The insert Venn-diagram illustrates private and shared alleles between the two species. (C) Distribution plot of heterozygosity levels among the two cell lines in each species. The horizontal line denotes the mean heterozygosity. (D) Ancestry coefficient plot of the eight cell lines. Mountain hare contribution to the ancestry in blue and brown hare in yellow. (E) Heatmap clustering of the eight cell lines based on the relative expression levels of the 16,689 orthologous genes. (F) PCA plot based on the relative expression levels of all 519,066–549,582 transcripts. (G) PCA

plot based on the relative expression levels of the 16,689 orthologous transcripts. LE = *Lepus europaeus*, LT = *Lepus timidus*.

Fig. 2. Species specific gene expression in hare fibroblasts. (A) Examples of differentially expressed GO-terms between the two species. (B) Volcano plot of results from the differential expression analyses on 16,689 orthologous genes. The vertical blue line indicates 2-fold difference and horizontal the *p*-value of 0.001. Some example genes are indicated.

Fig. 3. Comparison of the main mitochondrial parameters between mountain hare and brown hare cell lines. (A) Mitochondrial mass. FCCP is an uncoupling chemical used as a control to show that the mitochondrial staining works. Species effect: $p = 0.83$ and 0.82 (FCCP treated). (B) Mitochondrial membrane potential. Inverse gaussian model: Signal ~ Species/Cell line. Species effect: $p = 4\times10^{-12}$. (C) Comparison of cell respiration rates. (D) Explanation of the experimental conditions for (C). (E) Mitochondrial DNA (mtDNA) copy number and levels of example mitochondrial proteins as quantified from Western blots. Species effect: $p = 5.6\times10^{-3}$ (COX4); 0.11 (SDHA); 0.058 (TOM20); 0.19 (VDAC). Data are presented as mean ± SD; *$p < 0.05$; **$p < 0.01$; ***$p < 0.001$. LE = *Lepus europaeus*, LT = *Lepus timidus*.

Fig. 4. Cell proliferation and migration. (A) Cell doubling times in high and low glucose media (nuclear counting). Species effect: $p = 3.2\times10^{-3}$ (high glucose) and 3×10^{-7} (low glucose). (B) Delay time before the wound closure starts (left) and final wound closure rate (right). Species effect: $p = 0.027$ and 2.4×10^{-4} respectively. (C) Example image of a wound closure assay showing notable cell proliferation and migration after 21 h. Data are presented as mean ± SD; *$p < 0.05$; **$p < 0.01$; ***$p < 0.001$.

Fig. 5. Cell cycle comparison between mountain hare and brown hare fibroblasts. (A) Cell cycle phase distribution in the two species before and after synchronization. (B) Comparison of G1, S and G2 phase duration. Species effect: $p = 0.77$ (G1 phase); 1.09×10^{-3} (S phase); 4.5×10^{-6} (G2 phase). Species × time interaction: $p = 0.19$ (G1 phase); 6.1×10^{-3} (S phase); 0,79 (G2 phase). Data are presented as mean ± SD.

Fig. 6. Examples of the size and morphology of the cell lines. See S-Fig. 7 for more details.

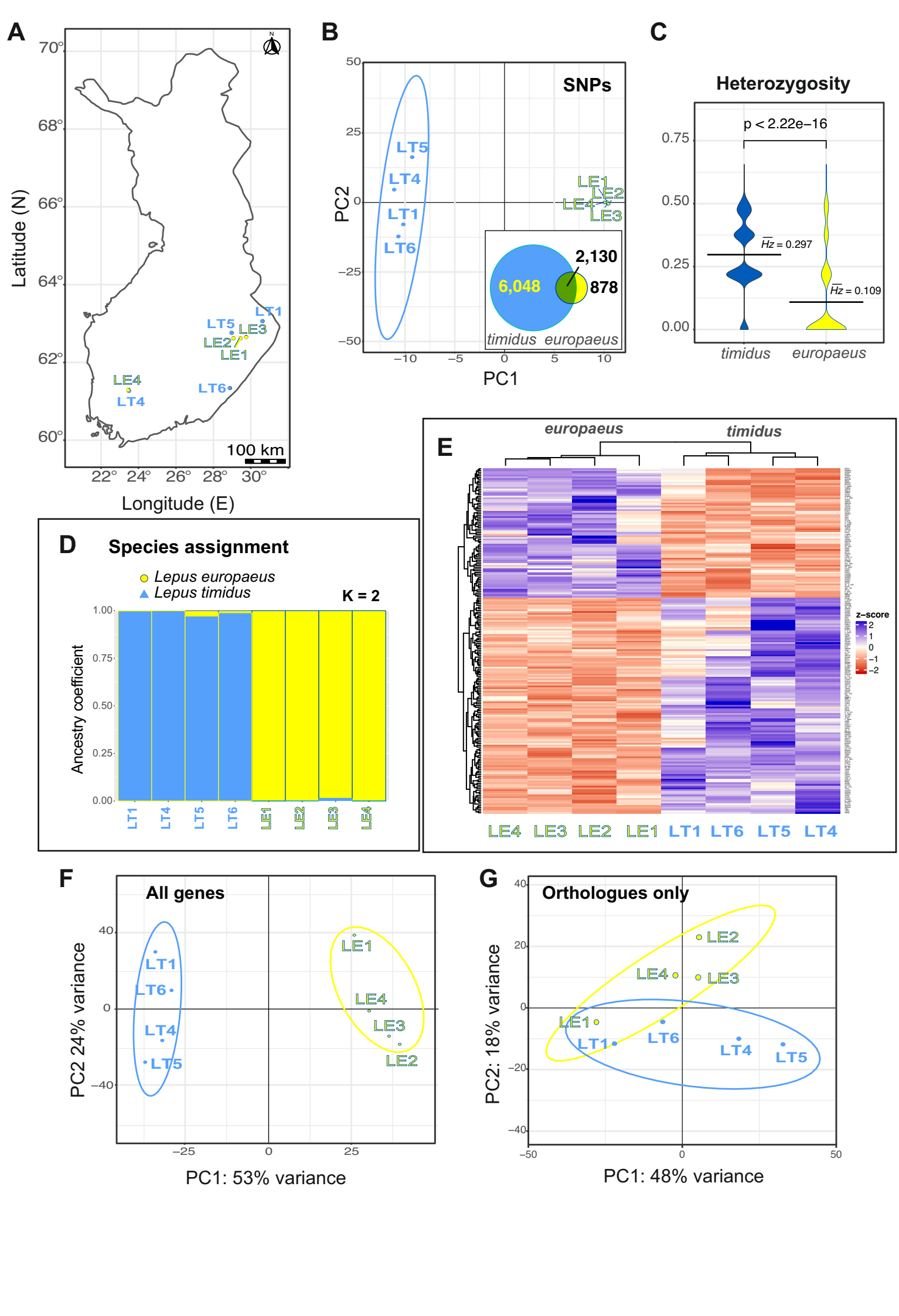
A
70°
68°
66°
64°
62°
60°
Latitude (N)
22° 24° 26° 28° 30°
Longitude (E)
100 km
LT1
LT5
LE3
LE2
LE1
LE4
LT4
LT6
B
SNPs
PC2
PC1
50
25
0
−25
−50
−10 −5 0 5 10
LT5
LT4
LT1
LT6
LE1
LE2
LE4
LE3
2,130
6,048
878
timidus europaeus
C
Heterozygosity
p < 2.22e−16
0.75
0.50
0.25
0.00
Hz = 0.297
Hz = 0.109
timidus
europaeus
D
Species assignment
Lepus europaeus
Lepus timidus
K = 2
Ancestry coefficient
1.00
0.75
0.50
0.25
0.00
LT1 LT4 LT5 LT6 LE1 LE2 LE3 LE4
E
europaeus
timidus
z−score
2
1
0
−1
−2
LE4 LE3 LE2 LE1 LT1 LT6 LT5 LT4
F
All genes
PC2 24% variance
40
0
−40
−25 0 25
PC1: 53% variance
LT1
LT6
LT4
LT5
LE1
LE4
LE3
LE2
G
Orthologues only
PC2: 18% variance
40
20
0
−20
−40
−50 0 50
PC1: 48% variance
LE2
LE4
LE3
LE1
LT1
LT6
LT4
LT5

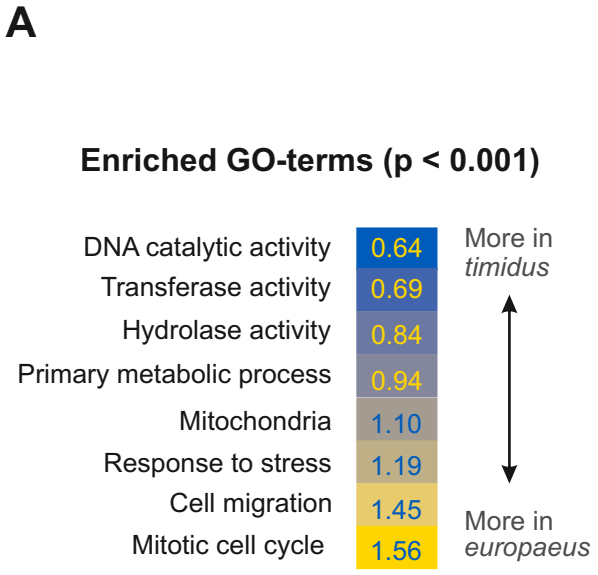
A
Enriched GO-terms (p < 0.001)
DNA catalytic activity
Transferase activity
Hydrolase activity
Primary metabolic process
Mitochondria
Response to stress
Cell migration
Mitotic cell cycle
0.64
0.69
0.84
0.94
1.10
1.19
1.45
1.56
More in timidus
More in europaeus

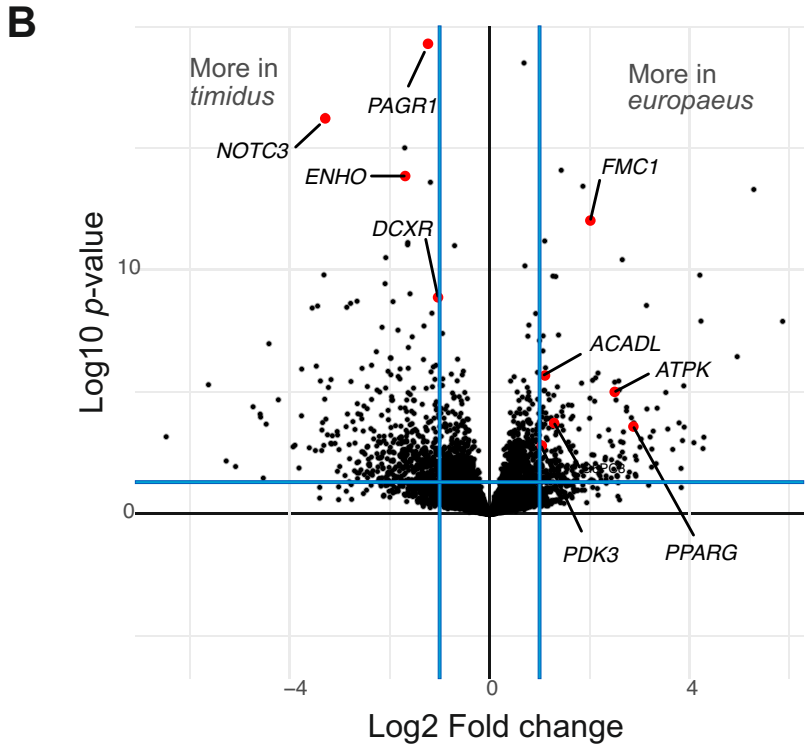
B
More in timidus
More in europaeus
PAGR1
NOTC3
ENHO
DCXR
FMC1
ACADL
ATPK
PDK3
PPARG
Log10 p-value
10
0
−4
0
4
Log2 Fold change

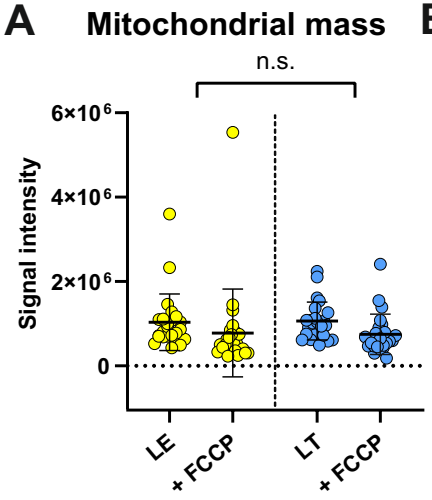

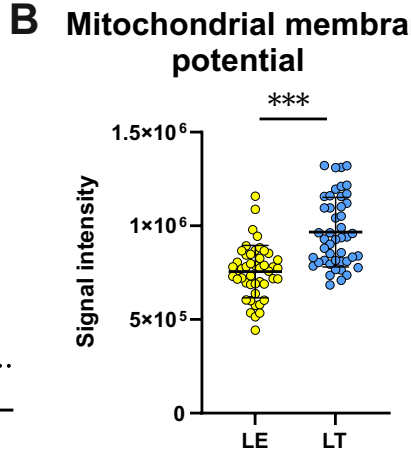

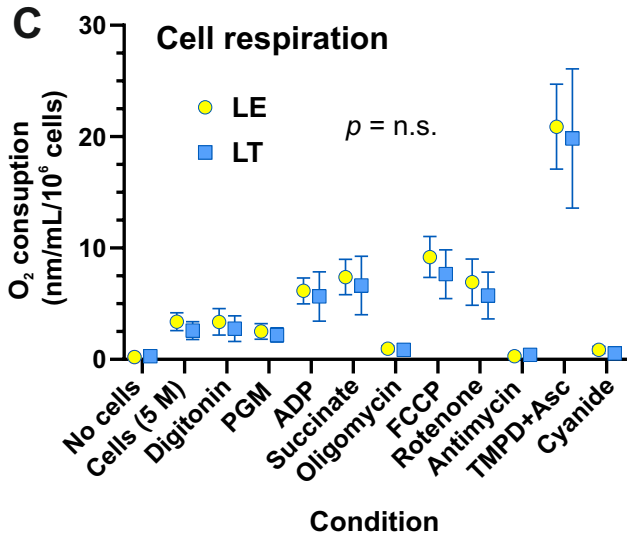

D

Condition	Role	Effect	Mitochondrial state
Cells			
Digitonin	Detergent	Cell permeabilisation	Basal mitochondrial respiration (state 1)
PGM = Pyruvate, Glutamate & Malate	Substrates	Krebs cycle, CI and CII	Respiration with substrates (state 2)
ADP	Respiration driver	CII	Max physiological respiration (state 3)
Succinate	Substrate	CV	
Oligomycin	Inhibitor	CV	CV block
FCCP	Uncoupler	Uncoupling mitos	Max respiration
Rotenone	Inhibitor	CI	CI block
Antimycin A	Inhibtior	CIII	CIII block
TMPD	Susbstrate	CIV (electron carrier)	Maximum CIV respiration
Ascorbate (Asc)	Substrate	CIV (electron donor)	
Cyanide	Inhibitor	CIV	CIV block

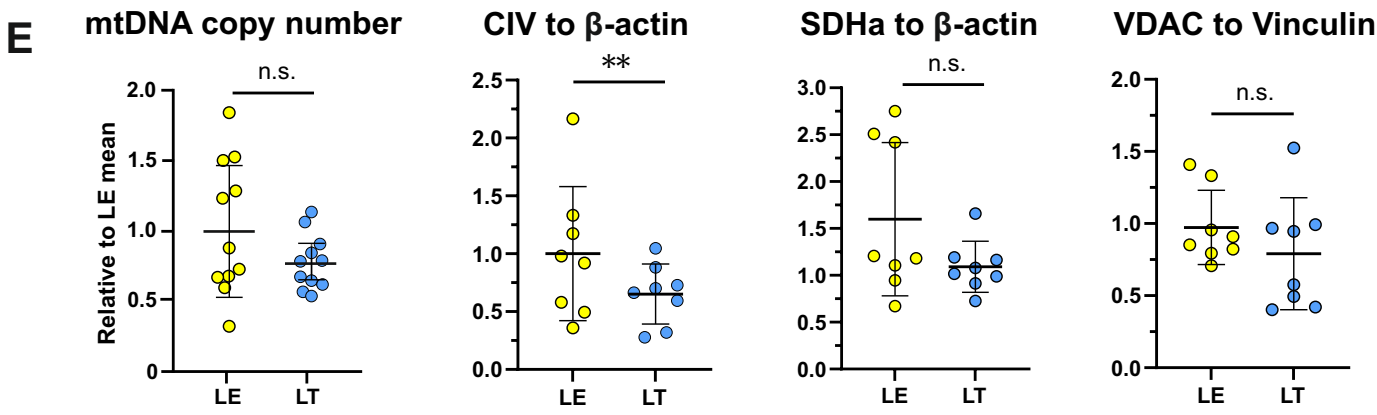

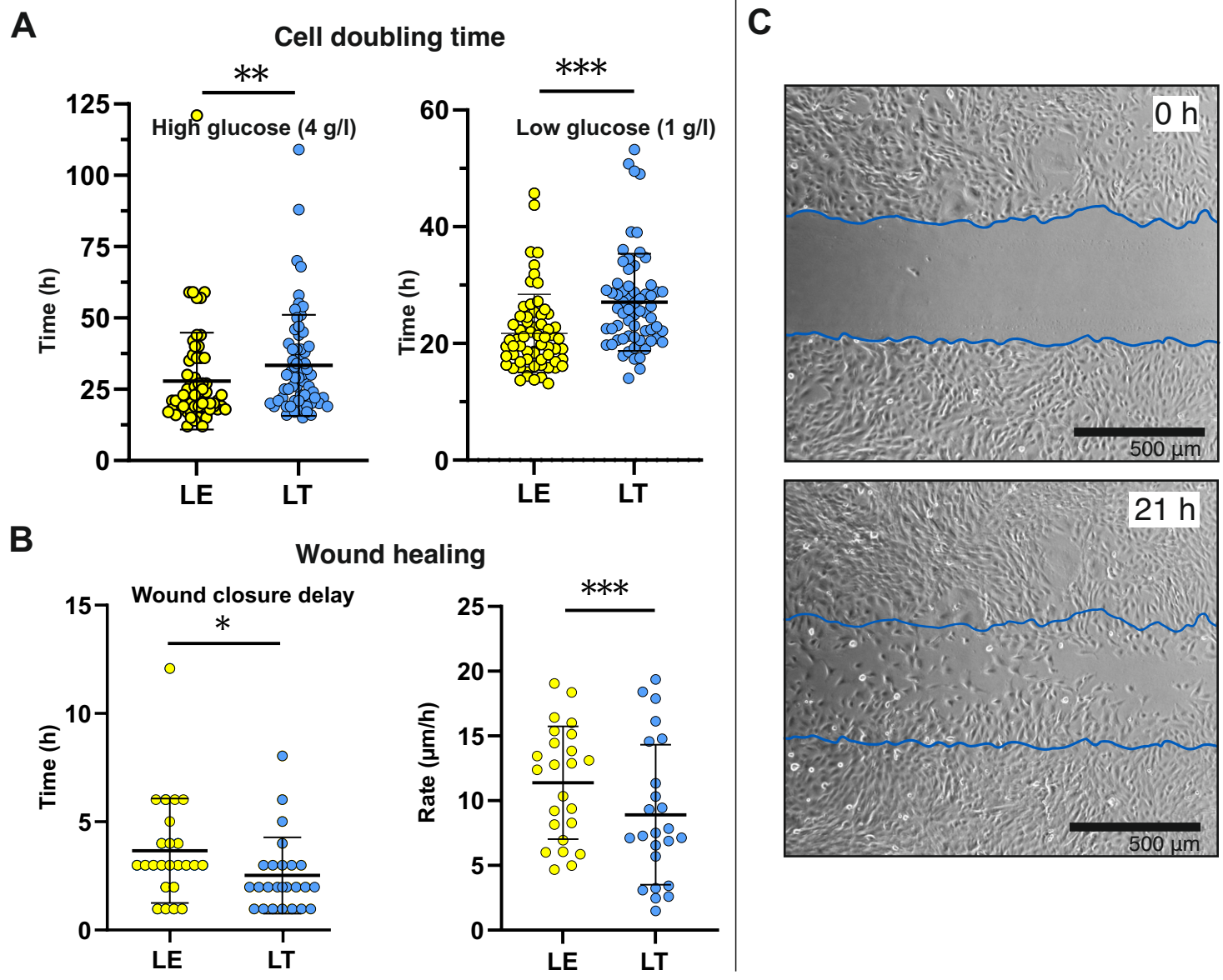
A
Cell doubling time
**
***
High glucose (4 g/l)
Low glucose (1 g/l)
Time (h)
125
100
75
50
25
0
60
40
20
0
LE
LT
B
Wound healing
Wound closure delay
*
***
Time (h)
Rate (µm/h)
15
10
5
0
25
20
15
10
5
0
LE
LT
C
0 h
500 µm
21 h
500 µm

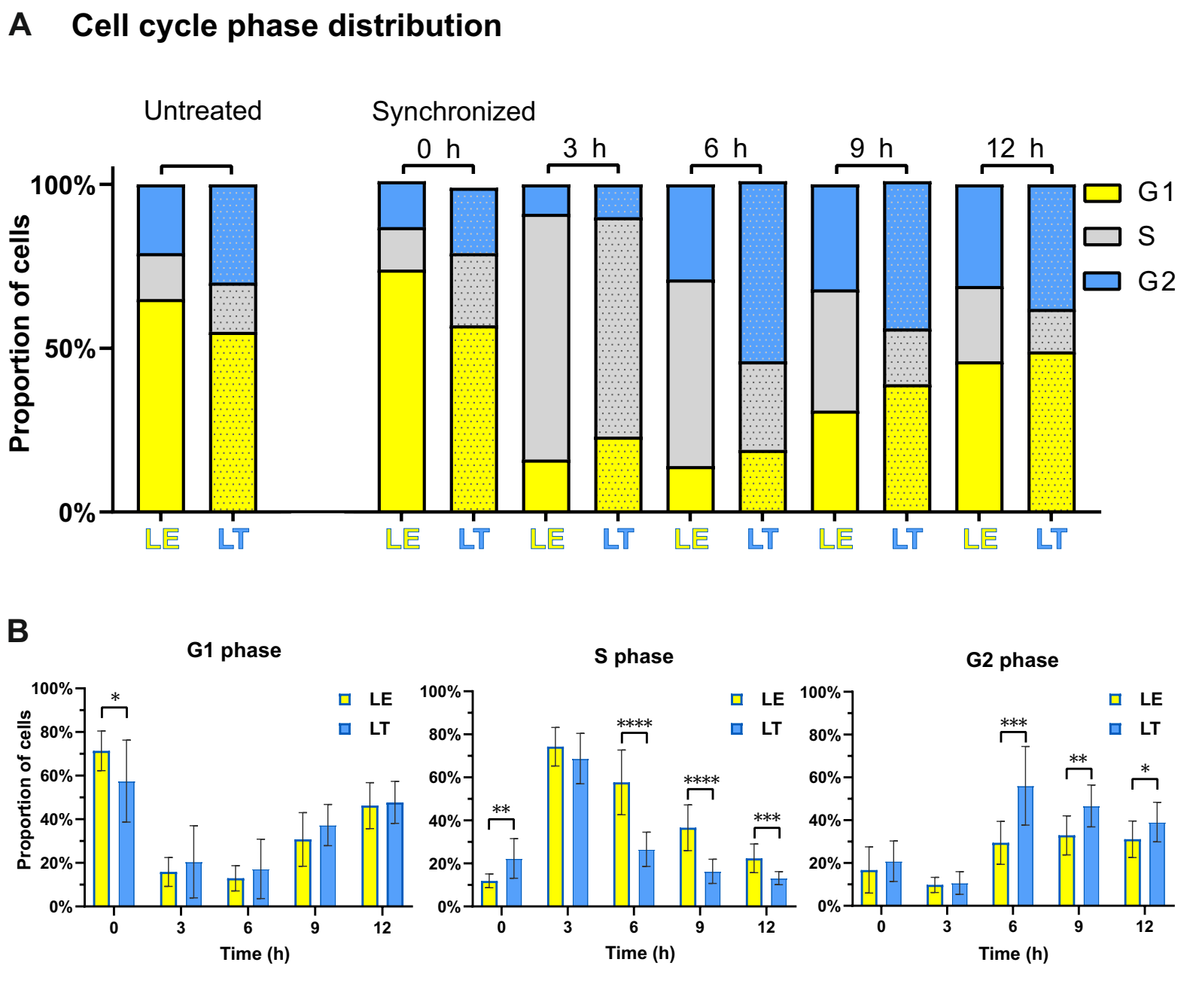
A
Cell cycle phase distribution
Untreated
Synchronized
0 h
3 h
6 h
9 h
12 h
100%
50%
0%
Proportion of cells
G1
S
G2
LE
LT
B
G1 phase
S phase
G2 phase
Time (h)

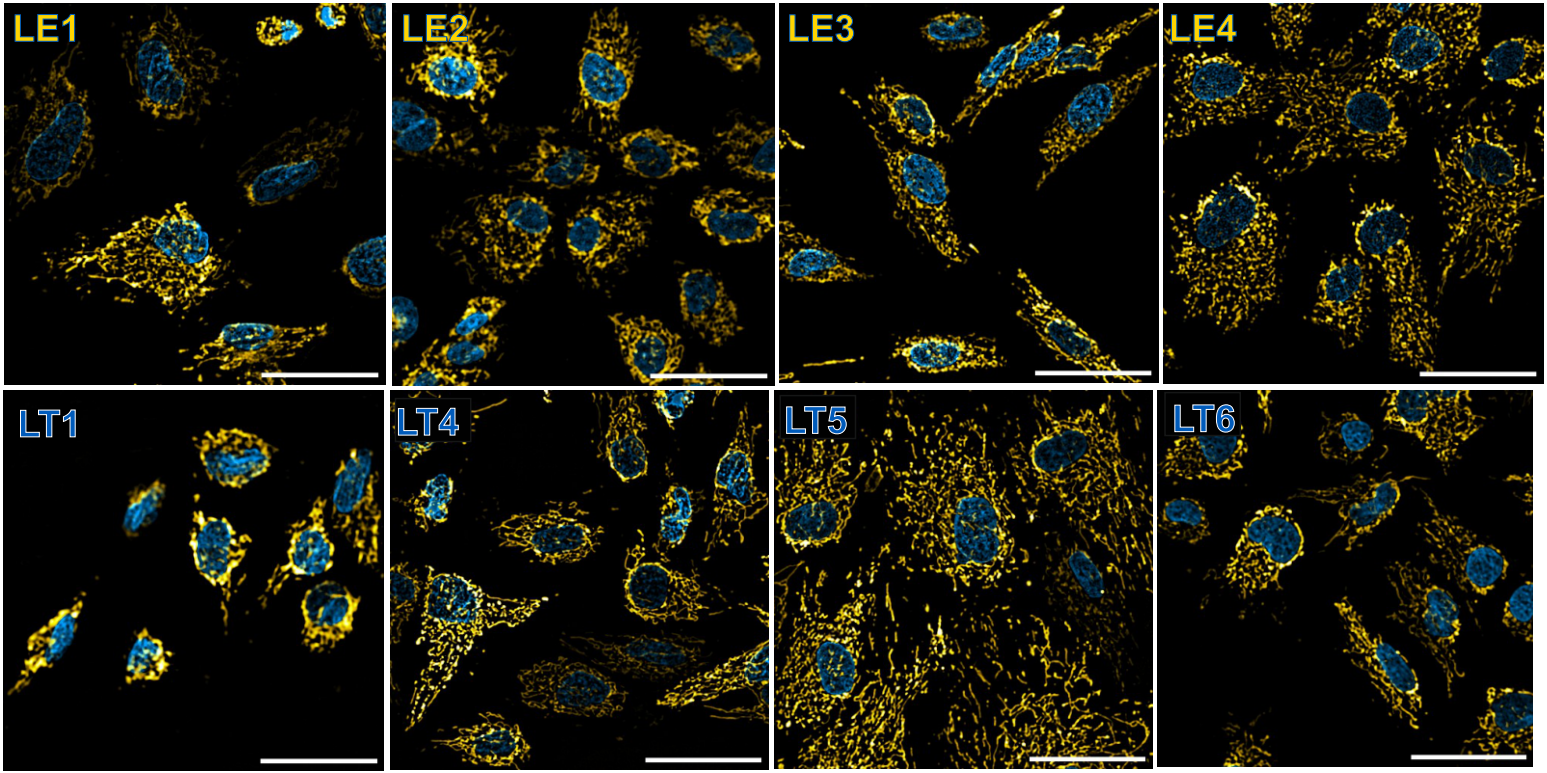
LE1
LE2
LE3
LE4
LT1
LT4
LT5
LT6

MOLECULAR ECOLOGY

Supplemental Information for:

Molecular phenotyping uncovers differences in basic housekeeping functions among closely related species of hares (Lepus spp., Lagomorpha: Leporidae)

Kateryna Gaertner[1]‡, Craig Michell[2,3]‡, Riikka Tapanainen[2], Steffi Goffart[2], Sina Saari[1], Manu Soininmäki[2], Eric Dufour[1]‡ and Jaakko L. O. Pohjoismäki[2]†‡

†Corresponding author
‡These authors contributed equally

[1]Mitochondrial Bioenergetics and Metabolism, Faculty of Medicine and Health Technology, FI-33014 Tampere University, Finland
[2]Department of Environmental and Biological Sciences, FI-80101 University of Eastern Finland, Finland
[3]Red Sea Research Center, Division of Biological and Environmental Science and Engineering, King Abdullah University of Science and Technology (KAUST), Thuwal, Saudi Arabia

Table of contents:

MOLECULAR ECOLOGY

Supplementary methods

Sampling

The specimens were instantly killed using 12/76-gauge shotguns with 40 g charge, lead-free 2.75 mm tungsten (UnA) shells or a .22WMR rifle with 1.92 g Hornady V-Max® ammunition at a maximum distance of 40 m. The sampling had minimal impact on the populations and no impact on their habitats. Because both species are legal game animals in Finland and the hunting followed the regional hunting seasons and legislation (Metsästyslaki [Hunting law] 1993/615/5§), the sampling adheres to the ARRIVE guidelines and no ethical assessment was required. The sampling had minimal impact on the populations and no impact on their habitats. Sampling did not involve International Trade in Endangered Species of Wild Fauna and Flora (CITES) or other export of specimens, as defined by the Convention on Biological Diversity (CBD).

Generation of immortalized fibroblast cell lines

A 3 mm × 5 mm piece of abdominal skin was removed and placed in a 15 ml vial with high glucose Dulbecco's Modified Eagle Medium (DMEM, Biowest), supplemented with 10 % fetal bovine serum and 100 μg/ml Primocin® antimicrobial agent (InvivoGen, Toulouse France). Samples were kept at ambient temperature until arrival at the laboratory, generally within 48h of the sampling. The skin biopsies were cut by scalpel into smaller pieces, placed on 35 mm cell culture dishes with DMEM containing fetal bovine serum and Primocin and incubated at 37 °C, 100 % humidity and 7,5 % CO_2. After 4-5 days, the skin pieces were removed, and the growth medium changed to DMEM containing Penicillin and Streptomycin. Fibroblasts attached to the cell culture plate were cultivated until ca. 70 % confluence and then transfected with a mammalian expression vector containing the large T-antigen gene (Addgene #21826), using Lipofectamine 3000 according to the manufacturer's instruction. When reaching full confluence, the fibroblasts were reseeded at 5 % confluence. After six such passages the fibroblast cell lines (i.e., one cell line per animal) were frozen as liquid nitrogen stocks. Cells used for the experiments were derived from these stocks to minimize genotypic drift under culture conditions.

Cell culture

Fibroblasts were maintained under standard cell culture conditions at 37°C, 5% CO2 in a humidified incubator. Cells were grown in high-glucose (HG, 4.5 g/l) or low-glucose (LG, 1 g/l) Dulbecco's modified Eagle's medium (DMEM, Sigma-Aldrich, #D6546 and #D5546 respectively). Media were supplemented with 10% heat inactivated fetal bovine serum (Sigma-Aldrich, # F7524), 1% L-glutamine, and 1% penicillin–streptomycin. For cell dissociation 1x trypsin–EDTA (Gibco, # 15400054) was used. Cell concentrations were measured using an EVE™ automatic

cell counter. Cell passaging was performed by trypsine dissociation, when the cells approached 70-95% confluence. A random sample of one million cells from the dissociated cell population was plated on the new culture plate(s).

RNA isolation and sequencing

Total RNA was extracted from each of the eight hare cell lines using TRI-Reagent® (Sigma-Aldrich) according to the manufacturer's instruction and quantified by NanoDrop. Poly(A)+ mRNA was extracted from the total RNA using the NEBNext® Poly(A) mRNA Magnetic Isolation Module (Item Number: E7490S, NEB) following the manufacturer's protocol. Sequencing was performed on the NovaSeq 6000. The sequencing libraries were prepared using the Illumina TruSeq stranded mRNA library preparation kit (Item Number:20020594, Illumina) and then 2x150bp paired end sequenced on the Illumina NovaSeq using a S1 flowcell with v 1.5 chemistry.

De novo transcriptome assembly

Sequencing adapters and low quality base pairs were trimmed and removed using Trimmomatic version 0.39 (Bolger, Lohse, & Usadel, 2014) with the following options enabled: ILLUMINACLIP: TruSeq3-PE.fa:2:30:10:2:keepBothReads; LEADING:5; TRAILING:5; MINLEN:50. The trimming of the reads was confirmed and inspected using FastQC version 0.11.8 (Andrews, 2010) followed by multiQC version 1.10.1 (Ewels, Magnusson, Lundin, & Kaller, 2016) to compile the data.

De novo transcriptome assemblies were created for each species using Trinity version 2.13.0 (Haas et al., 2013) on the Puhti server of the Center for Scientific computing Finland (CSC). Prior to assembly the reads from the four biological replicates were combined to increase the diversity of the final transcriptome assembly. Then Trinity was run with the following parameters: --seqType fq; --max_memory 124G; --left Letim.P1.fastq.gz; --right Letim.P2.fastq.gz; --SS_lib_type RF; --CPU 8; --normalize_max_read_cov 100; --full_cleanup; --output trinity_run_out; --grid_exec sbatch_commandlist_trinity. After the transcriptome assembly, the assembly statistics were calculated using TrinityStats.pl.

Validation and transcriptome filtering

The trimmed reads used to assemble the transcriptome were mapped back on to their respective assembly using bowtie2 version 2.4.4 (Langmead & Salzberg, 2012). As a large number of transcripts were assembled for each species, we used three different filters to reduce the number of misassembled and poor-quality transcripts in the data. Firstly, we removed lowly expressed genes from the transcriptomes using the align_and_estimate_abundance.pl (Li & Dewey, 2011) and filter_low_expr_transcripts.pl scripts

included with the Trinity package. Secondly, we reduced the redundancy of the transcriptomes by clustering similar transcripts at 95% similarity with CD-HIT version 4.8.1 (Fu, Niu, Zhu, Wu, & Li, 2012). Finally, miss-assembled and incomplete transcripts were removed from the transcriptomes using TransRate version 1.0.3 (Smith-Unna, Boursnell, Patro, Hibberd, & Kelly, 2016).

Completeness of the transcriptomes was assessed by identifying and comparing single copy orthologs from the transcriptomes against the general (Metazoa_odb10, Download date: 2021-02-17) and lineage specific (Glires_odb10, Download Date: 2021-02-19) databases using BUSCO version 5.2.2 (Waterhouse et al., 2018).

Functional annotation of transcriptomes

The functional annotation of the transcriptomes was performed following the Trinotate pipeline (Bryant et al., 2017). TransDecoder version 5.5.0 was used to identify open reading frames with a minimum length of 200 amino acids (-m 200). The identified transcripts and predicted proteins were compared against the SwissProt protein database using diamond version 2.0.4.142 with the parameters: --max-target-seqs 1; --outfmt 6; --more-sensitive. Protein domains, signal proteins and transmembrane proteins were mined from the protein sequences using hmmer version 3.1 (Finn, Clements, & Eddy, 2011), SignalP version 4.1 (Petersen, Brunak, von Heijne, & Nielsen, 2011) and, tmhmm version 2.0 (Krogh, Larsson, von Heijne, & Sonnhammer, 2001) respectively. RNAmmer version 1.2 (Lagesen et al., 2007) was used to identify rRNA genes in the transcriptome using the wrapper script RnammerTranscriptome.pl provided in the Trinotate pipeline. For each species, the output from each analysis was compiled in the Trinotate SQlite database.

Transcript genotyping

Genetic variants were identified by mapping the reads onto the pseudo-reference genome (Genbank accession: GCA_009760805.1) (Marques et al., 2020) using STAR version 2.7.8 (Dobin et al., 2013). Variants were then called following the recommendation of the GATK 4.0 pipeline for RNAseq data (Brouard, Schenkel, Marete, & Bissonnette, 2019). The raw variant file was filtered using VCFtools (Danecek et al., 2011). Following the removal of indels, missing data, and variants with an MAF < 0.05, we obtained 1 biallelic site for each contig. The resulting VCF file was analyzed for basic population genomic parameters using Poppr2 (Kamvar, Tabima, & Grunwald, 2014). The ancestry coefficient of each sample was estimated using the sparse non-negative matrix factorization (sNMF) method in LEA (Frichot & Francois, 2015).

DNA isolation, sexing, mtDNA genotyping and DNA copy number analysis

Total DNA was extracted from the cells using the peqGOLD Blood and tissue DNA mini kit (VWR Life Science). Primers and TaqMan™ probes (Metabion International AG, Panegg, Germany) were designed to be fully compatible for both species, targeting the *16S* gene of the mtDNA as well as *SDHa* for the single-copy nuclear locus:
Lepus-16S-F: 5´-ACC CCG CCT GTT TAC CAA-3´
Lepus-16S-R: 5´-ATG CTA CCT TTG CAC GGT CA-3´
Lepus-16S-probe: 5´-6-Fam-TGC CTG CCC AGT GAC AAA CGT-BHQ-1-3´
Lepus-SDHa-F: 5´-CCT GCC TGG CAT TCC TGA GA-3´
Lepus-SDHa-R: 5´-ATT GGC TCC TTG GTG ACG TC-3´
Lepus-SDHa-probe: 5´-Hex-GCC ATG ATC TTC GCG GGT GTG-BHQ-1-3´
The qPCR program had an initial denaturation step of 3 min 95 °C followed by 40 cycles of 15 s 95 °C, 15 s 54 °C and 15 s 72°C (read).

Differential gene expression

Transcripts identified as reciprocal best BLAST hits as determined by the bit score (python script available on request) were then extracted from the final transcriptomes into species-specific fasta files. Trimmed reads for all samples were mapped onto the one-to-one reciprocal best BLAST hits of *L. timidus* and then *L. europaeus* using bowtie2 version 2.4.4 with the following parameters --all --min-score L,-0.1,-0.1. Clustering and quantification was done using Corset version 1.09 (Davidson & Oshlack, 2014). Differentially expression analysis was done using the Integrative Differential Expression Analysis for Multiple Experiments (IDEAMEX) webtool (Jimenez-Jacinto, Sanchez-Flores, & Vega-Alvarado, 2019). Visualization of the RNAseq was then performed in R using ggplot2 (Ginestet, 2011).

Cell growth measurements

Nuclei counting

Cells were seeded into 48 well plates at 3×10^3 cells/well, in quadruplicate. Fibroblasts were fixed in 4% paraformaldehyde (PFA) (RT, 20 min.), washed with 1× Dulbecco's Phosphate Buffered Saline (PBS) and stained in 1 µg/ml Hoechst solution (Invitrogen, # H1399, RT, 10 min.). Cells were rinsed twice with 1× PBS before imaging with an Olympus IX51 Inverted Phase Contrast Fluorescence Microscope (DAPI filter, EM 420, EX 360/370, 1 sec. exposure). For each well, four images, aligned alongst the longest width, were captured at 10 × magnification with an interval of one visual field between each image. Images were processed in Fiji-ImageJ-64bit software (Rasband, W.S., ImageJ, U. S. National Institutes of Health, Bethesda, Maryland, USA, https://imagej.nih.gov/ij/, 1997-2018). Nuclei were separated from the background by thresholding. Clumped nuclei were split by applying Watershed algorithm. Automatic particle

counting was applied to count nuclei excluding partial nuclei at the images' edges and debris.
Missing data: None.
Statistical analysis: Analysis was performed using the growth slopes as the response variable. The slope was obtained from the ln (nuclei count) = $f_{(t)}$ function. The logarithm conversion allowed to verify the data quality. PDT was not used for the statistics since one slope had a null coefficient leading to infinite PDT (LT6 sample 4). The predictor was the species (with cell line nested into the species): slope ~ species/cell line. The data best fitted a gamma distribution for high glucose condition and gaussian distribution for low glucose condition. The difference is likely due to the presence of negative slopes in low glucose conditions.

Cell counting
Plates were placed into the onstage incubator of EVOS® FL cell imaging system adjusted to the standard culture conditions. Cells were manually counted in each image using the multi-point tool from Fiji-ImageJ.
Missing data: Sample 12 from LT6 was lost.
Statistical analysis: analysis was performed as described for the nuclei counting. A gaussian distribution model was best fitting both low and high glucose condition.

Cell cycle measurements
Cells were blocked in the G1 to S phase transition by incubation for 18 hours in the presence of aphidicolin (2.5 µg/ml of in growth medium) (Sigma-Aldrich, # A0781) except for the control wells. To resume cell cycle progression, aphidicolin-containing medium was removed by washing with 1× PBS and replaced by fresh growth medium. Every three hours starting from T_0 (removal of aphidicolin), samples from three wells were collected at a density of 1×10^6 cells/ml and ethanol fixed (70% ethanol in ice-cold 1× PBS) for 24 h at +4°C. Samples were then rinsed with ice-cold 1× PBS, treated with RNase A (1 mg/ml in 10 mM Tris-HCl, pH 7.5, 15 mM NaCl; RNASEA-RO, Roche) at 37°C for 30 min and stained for 30 min at room temperature, in the dark, with 10 µg propidium iodine (PI; 20 µg/ml in 1× PBS) per 1×10^6 cells (Sigma-Aldrich, #P4864). PI staining was analysed from 2×10^4 events per sample (EX 561 /EM 585) using Cytoflex S Flow Cytometer. Cycling cells were gated using the area and hights of the PI channel using CytExpert software to exclude doublets and prevent G2 overestimation. The number of cells in G1, S, and G2 phases were calculated from the histogram of cell count vs PI staining area after visually inspection for accuracy.
Missing data: LE3 measure 2, time 0; LE3 measure 3 time 12 and LT5 measure 3 time 12 (sample damaged).
Statistical analysis: Each phase of the cell cycle was analyzed separately. The role of the species and time × species predictors during each phase of the cycle were compared to obtain a global assessment of the differences in the cell cycle progression between the two species. Analysis was performed using the number cell in the phase of the cycle analyzed as the response variable, weighted by the total cell count. The predictors were the species (with cell line nested into the species) and the time after release of the cell cycle block. A negative binomial

distribution and full interaction model (response variable ~ Species/Cell_line × Time) were best fitting the three cell cycle phases. Comparisons of the cell lines within species were performed with one-way ANOVA (S-Figs. 1–4, 6, 8, 9 & 11).

Wound healing assay

Manual scratching was performed with a sterile 200 µl micropipette tip to produce a linear cell-free zone in the centre of each well. Cells were washed with 1× PBS to remove debris, and fresh growth medium was added. Each plate was maintained in the microscope stage of either an EVOS® FL (repeat 1) or a Cell-IQ® (repeat 2) automatic cell imaging system adjusted to the standard cell culture conditions. For each well, three phase contrast images were captured at 4 × magnification with 1 h interval for 48 h. The length of the wound (*l*) was measured using a straight-line selection tool in Fiji-ImageJ software. Wound areas were quantified at each time point using MRI Wound Healing tool (Volker Baecker, Montpellier RIO Imaging, Montpellier, France). For each series of images, the wound area *versus* time was plotted. Comparative R-Squared analysis was used to define the longest time interval during which cell migration was linear. Slope values were extracted from the linear function and converted into wound closure rate ($WCR = \frac{|slope|}{2*l}$).

Missing data: None.

Statistical analysis: analysis was performed using (1) the wound closure rate and (2) the wound closure delay as the response variable. In both cases, the predictors were the species (with cell line nested into the species) and the instrument (EVOS vs CellIQ) used. We tested models without interaction between instruments and species, as such interactions would have no biological rationale. A gamma distribution was used for both response variables.

Mitochondrial mass measurements

Cells were collected and resuspended in 1× PBS at 1×10^6 cells/ml. Aliquots of 0.5×10^6 cells were made. Staining was performed exposing cells suspensions to 25 nM NAO (nonylacridine orange; Invitrogen, #A1372) under otherwise standard culture conditions for 20 min. To demonstrate that NAO staining is dependent on the mitochondrial membrane potential, uncoupling was performed with FCCP (50 µM, 3 min) prior to NAO staining. Intensity of NAO staining was measured from 2×10^4 events per sample (EX 488 /EM 525) in a Cytoflex S Flow Cytometer. Data was processed in FlowJo™ software (Version 10.7.2. Ashland, OR: Becton, Dickinson and Company; 2021) excluding cell-doublets from the analysis. From the resulting NAO signal intensities outliers were removed using the ROUT method (FDR: 1%) (Motulsky & Brown, 2006).

Missing data: None.

Statistical analysis: analysis was performed using NAO intensity per cell as the response variable. Cells treated with FCCP and untreated cells were analyzed separately. In both cases, the predictor was the species (with cell line nested into the species). In both cases, an inverse gaussian distribution was used, since it fitted best the response variables.

Mitochondrial membrane potential measurement

Staining was performed in the presence of 50 µM Verapamil (Sigma-Aldrich, # V4629) (Morganti, Bonora, Ito, & Ito, 2019). Fibroblasts were stained with TMRM (tetramethylrhodamine, methyl ester, 20 nM, Invitrogen, # T668) under standard cell culture conditions for 30 min. When needed, MMP was collapsed by FCCP (50 µM, 3 min). When needed, MMP was allowed to reach its maximum level using Oligomycin treatment (5 µg/mL, 3 min) before TMRM staining. Untreated cells were used as negative controls. The intensity of TMRM staining was measured from 2×10^4 events per sample (EX 561 /EM 585) with Cytoflex S Flow Cytometer. Cell-doublets were excluded from the analysis using FlowJo software. TMRM fluorescence signal per cell line was calculated as (TMRM) – (TMRM + FCCP).
Missing data: LE4 measure 3, LT1 measure 3 and LT1 measure 6 (insufficient cell count).
Statistical analysis: Analysis was performed using corrected TMRM intensity ((TMRM) – (TMRM + FCCP)) per cell as the response variable. The predictor was the species (with cell line nested into the species). An inverse gaussian distribution fitted best the response variables.

Mitochondrial morphology

The 35mm glass bottom poly-d-lysine coated plates were obtained from MatTek, # P35GC-1.5-14-C. The growth medium was refreshed 1 hour before cell staining. Cells were incubated in MitoTracker Deep Red FM (50 nM, Invitrogen, cat. #M22426) + NucBlue (2 drops/ml, Invitrogen, #R37605) in growth medium at 37°C and 5% CO_2 for 10 min, then washed with PBS and maintained in 1× PBS during imaging. Imaging was performed using Olympus IX51 Inverted Phase Contrast Fluorescence Microscope at EX 360/70, EM 420, exposure time 1 s, to visualise cell nuclei, and EX 620/60, EM 700/75, exposure time 1 s, to image mitochondria. Images were processed in Fiji-ImageJ software.

Mitochondrial respiration measurements

For each measure, 5×10^6 cells were pelleted and resuspended in 550 µL of respiration buffer (225 mM Sucrose, 75 mM mannitol, 10 mM KCl, 10 mM KH_2PO_4, 5 mM $MgCl_2$, 10 mM TRIS pH 7.4, 1 mg/ml of bovine serum albumin BSA). Cell suspensions were immediately added into the oxygen-calibrated chamber of Hansatech Oxytherm respirometer. Cells were permeabilised with digitonin (55 µM). Mitochondrial respiration was assessed by additions of respiratory substrates and inhibitors to the sample in the following order: pyruvate + glutamate + malate (5 mM each, Sigma-Aldrich respectively #P8574, #G5889, #M7397), ADP (1 mM, Calbiochem #117105), succinate (5 mM, Sigma-Aldrich #W327700), oligomycin (1 µM, Sigma-Aldrich #75351), FCCP (1 µM, Sigma-Aldrich # C2920), rotenone (300 nM, Sigma-Aldrich #R8875), antimycin A (90 ng/ml, Sigma-Aldrich #A8674), ascorbate + N,N,N',N'-tetramethyl-p-phenylenediamine (700 µM, Sigma-Aldrich #A4034 + 300 µM, Sigma-Aldrich #T7394), and potassium cyanide (200 µM, Sigma-Aldrich #60178). Oxygen consumption ($pmol\times sec^{-1}\times ml^{-1}$) is presented per million of cells.
Missing data: One LE2 trace was unreliable due to extreme background noise and omitted from the analysis.

Protein preparation and Western blotting

Cells grown were collected by trypsinization, washed with ice-cold DPBS and lysed in ice-cold RIPA buffer (50 mM Tris, pH 8.0; 150 mM NaCl; 1% Triton X-100; 0.5% sodium deoxycholate; 0.1% sodium dodecyl sulfate) supplemented with cOmplete EDTA-free Protease Inhibitor Cocktail (Roche, # 04693132001). Samples were maintained on ice for 30 min and centrifuged at 13 000 × g and 4°C for 20 min. Protein supernatants were stored at -80 °C. Protein concentration was measured with BCA assay (Pierce BCA Protein Assay Kit, #23225) using an EnVision® 2105 (Abs. 562 nm) plate reader. 30 µg of protein per sample was loaded in Criterion™ TGX Stain-Free™ precast gels (Biorad, #5678093). Proteins were transferred onto nitrocellulose membranes (Biorad, #1704158, #1704159) using the Transblot-Turbo Transfer System (Biorad, #1704150). Blots were washed in Tris-buffered saline-Tween buffer (TBS-T) and blocked with TBS-T + 5% milk for 1 h under agitation at RT. Blots were probed at +4 ^{o}C overnight in blocking buffer with one of the following primary antibodies: beta-Actin IgG rabbit polyclonal (1:1000; NB600-505; Novus Biologicals), COX IV IgG rabbit polyclonal (1:2000; ab16056; Abcam), SDHA IgG1 mouse monoclonal (1:10000; ab14715; Abcam), Tom20 IgG2a λ mouse monoclonal (1:200; sc-17764; Santa Cruz), Vdac1 mouse monoclonal (1:1000; SAB5201374; Sigma-Aldrich), Vinculin mouse monoclonal (1:10000; V9264; Sigma-Aldrich). After incubation, blots were washed with TBS-T and exposed for 2 h at RT in the dark to the relevant peroxidase-labelled secondary antibody diluted in 2.5% milk TBS-T buffer: goat anti-rabbit IgG (1:10000; PI-1000; Vector Laboratories) or horse anti-mouse IgG (1:10000; PI-2000; Vector Laboratories). Blots were washed with TBS and incubated with SuperSignal West Femto Maximum Sensitivity Substrate (Thermo Scientific, #34096) for 5 minutes in the dark. Images were obtained with ChemiDoc XRS^{+} Imaging System (Biorad, #1708265) using auto-exposure. Band intensities were quantified in Image Lab software and normalised to the intensities of reference proteins (beta-Actin or Vinculin).
Missing data: None.
Statistical analysis: analysis was performed using $intensity_{prot\ of\ interest}$ / $intensity_{reference}$ as the response variable. The predictor was the species (with cell line nested into the species). Because of the small number of samples, models were not tested, instead a gaussian distribution was used for all four proteins of interest.

Statistical analysis

A systematic approach was developed for all cell biology analyses. All statistics were performed using R (v 4.2.1) and RStudio (2021.09.0 Build 351).
We analyzed the relationship between our response variable and our predictor of interest, the species in which the cell line is a nested factor: glm (response variable ~ species/cell_line). Interaction with other predictors (e.g Time in the case of cycle experiments) was analyzed and

reported. Potential confounders (like the type of measure instrument used) were included as addictive predictors, their effect was verified but is not reported.
To identify the best type of distribution, for each of the experiment we tested all the suitable distributions from the library of distribution from the Generalized Additive Models for Location Scale and Shape (gamlss v. 5.2, Rigby and Stasinopoulos 2005). Fitted distribution were ranked using corrected Generalised Akaike Information Criteria (GAIC, c = TRUE). The best three to six distributions were visually inspected (FitDist tool). The residuals were evaluated using quantile-quantile plot and Filliben correlation (plot tool) as well worm- plots (wp tool). Distributions with aberrant residuals were eliminated.
The best distribution compatible with generalized linear modeling (glm, glm.nb) was then selected. Models with two predictors:

- During the cell cycle, we wanted to see if the passage of time had different influences on the two species, and therefore Species:Time interactions were included in the models. In addition, the Species:Cell_line:Time interaction had essential influence on the model of the G2 phase and was therefore kept for the models of the three phases of the cell cycle.
- In contrast in the analysis of cell growth, we expected that the instruments had no species-specific effect (no Species:Instrument interaction) and compared the model with and without this interaction. AICc analysis supported the use of a model without interaction.

Finally, the importance of each predictor and eventual interaction was assessed using ANOVA (anova, test = “Chisq”). The key results are reported in the figure legends.

MOLECULAR ECOLOGY

Supplementary Tables

S-Table 1. RNA sequencing read counts and SRA accession numbers for the cell lines.

Species	Cell line ID	Raw reads (PE)	Trimmed reads (PE)	SRA accession number
Lepus timidus	LT1	121,730,308	112,751,292	SAMN27555144
	LT4	124,677,084	116,762,368	SAMN27555145
	LT5	81,927,034	75,606,128	SAMN27555146
	LT6	183,597,094	171,314,838	SAMN27555147
Lepus europaeus	LE1	269,577,848	250,703,284	SAMN27555148
	LE2	141,499,210	130,128,674	SAMN27555149
	LE3	188,717,244	174,701,744	SAMN27555150
	LE4	197,190,242	178,804,524	SAMN27555151

MOLECULAR ECOLOGY

S-Table 2. Transcriptome statistics for the cell lines. The number of genes corresponds to unique transcripts and includes all allelic variants. Transdecoder was used to find genes based on complete ORFs and does not include truncated sequences, which contribute to the orthologue gene count.

		Species	
		Lepus europaeus	*Lepus timidus*
Raw	Number of Genes	419,721	413,402
	Number of Transcripts	549,582	519,066
	Total assembled bases	499,766,067	445,061,170
	Contig N50	2,020	1,918
	Contig N50 - longest isoforms only	716	658
	GC content (%)	49.8	49.55
Highly expressed - longest isoform only	Retained (% of input retained)	419,721 (76.37)	413,402 (79.64)
	Contig N50	622	583
	GC content	47.93	47.71
CD-Hit-EST 95%	Retained (% of input retained)	408,827 (97.40)	404,443 (97.83)
	Contig N50	631	589
	GC content (%)	47.9	47.69
High quality contigs	Retained (% of input retained)	398,741 (97.53)	395,469 (97.78)
	Contig N50	639	596
	GC content (%)	47.89	47.67
Transdecoder "-m 200 amino acids" *	Number of ORFs	16,879	16,071
Reciprocal BLAST (orthologue count)	Number of 1:1 reciprocal BLAST hits	16,689	16,689

S-Table 3. Gene ontology (GO)-terms that showed significant ($p < 0.001$) difference between the brown hares and mountain hares. The table is provided as a separate file, S-Table_3.xlsx.

S-Table 4. DE table per orthologous transcript. The table is provided as a separate file S-Table_4.txt.

MOLECULAR ECOLOGY

Supplementary Figures

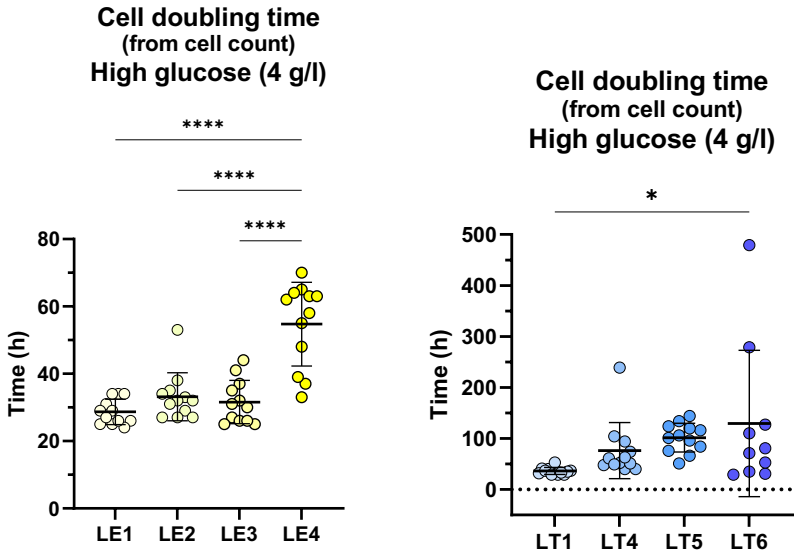

S-Fig. 1. Cell doubling time per cell line under high glucose conditions. Calculated from the cell count. *$p < 0.05$; ** $p < 0.01$; *** $p < 0.001$, **** $p < 0.0001$. One-way ANOVA. LE = *Lepus europaeus*, LT = *Lepus timidus*.

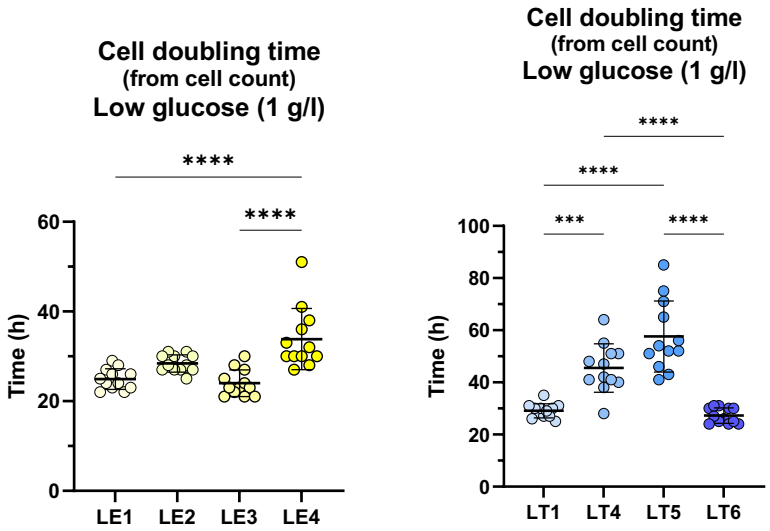

S-Fig. 2. Cell doubling time per cell line under low glucose conditions. Calculated from the cell count. *$p < 0.05$; ** $p < 0.01$; *** $p < 0.001$, **** $p < 0.0001$. One-way ANOVA. LE = *Lepus europaeus*, LT = *Lepus timidus*.

MOLECULAR ECOLOGY

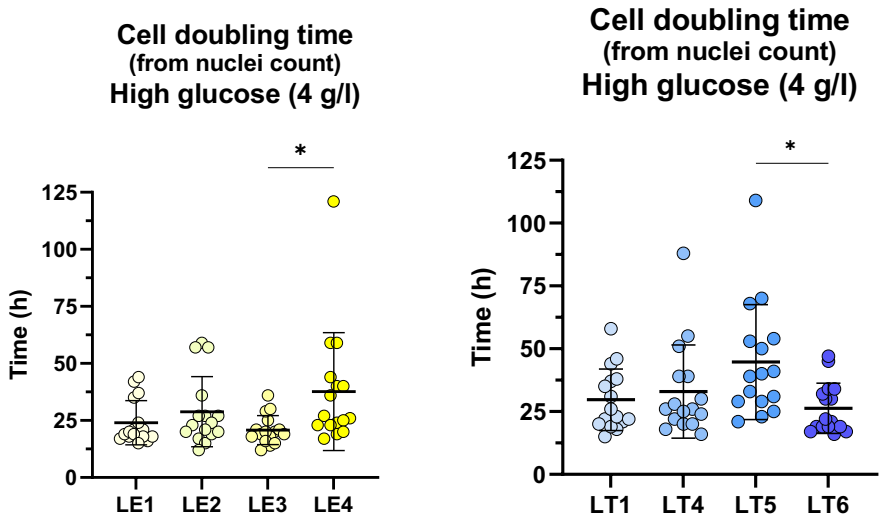

S-Fig. 3. Cell doubling time per cell line under high glucose conditions. Calculated from the nuclei count. *$p < 0.05$; ** $p < 0.01$; *** $p < 0.001$, **** $p < 0.0001$. One-way ANOVA. LE = *Lepus europaeus*, LT = *Lepus timidus*.

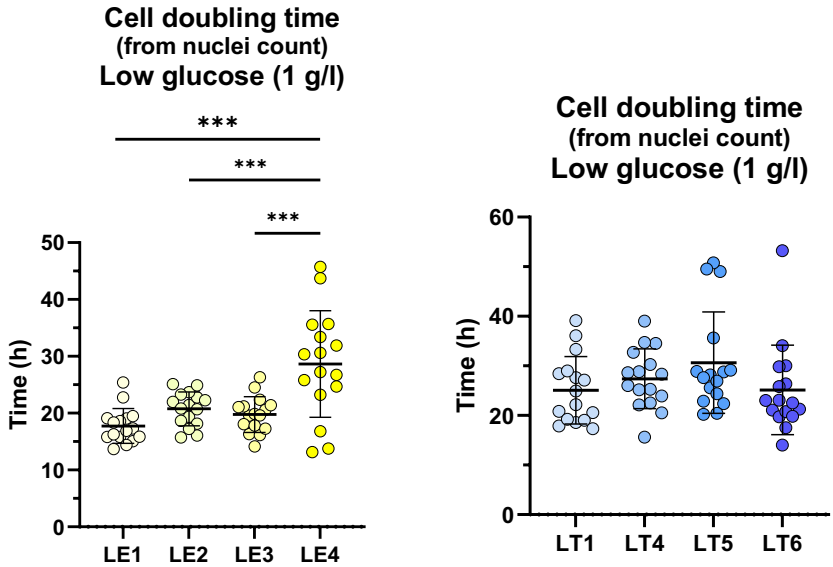

S-Fig. 4. Cell doubling time per cell line under low glucose conditions. Calculated from the nuclei count. *$p < 0.05$; ** $p < 0.01$; *** $p < 0.001$, **** $p < 0.0001$. One-way ANOVA. LE = *Lepus europaeus*, LT = *Lepus timidus*.

MOLECULAR ECOLOGY

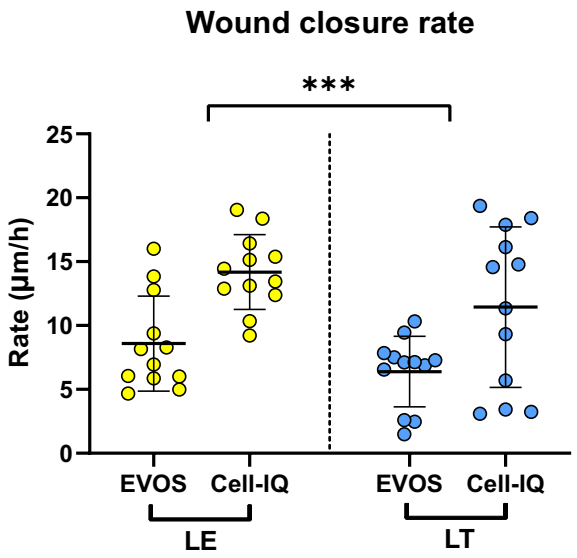

S-Fig. 5. Comparison of two instruments, EVOS and Cell-IQ, for the wound closure rate measurement. *$p < 0.05$; ** $p < 0.01$; *** $p < 0.001$, **** $p < 0.0001$. Nested. LE = *Lepus europaeus*, LT = *Lepus timidus*.

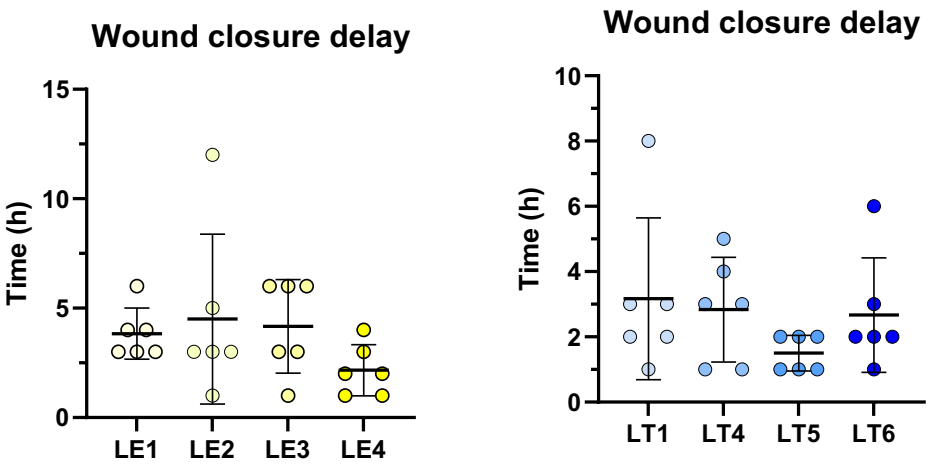

S-Fig. 6. Wound closure delay per cell line. One-way ANOVA. LE = *Lepus europaeus*, LT = *Lepus timidus*.

MOLECULAR ECOLOGY

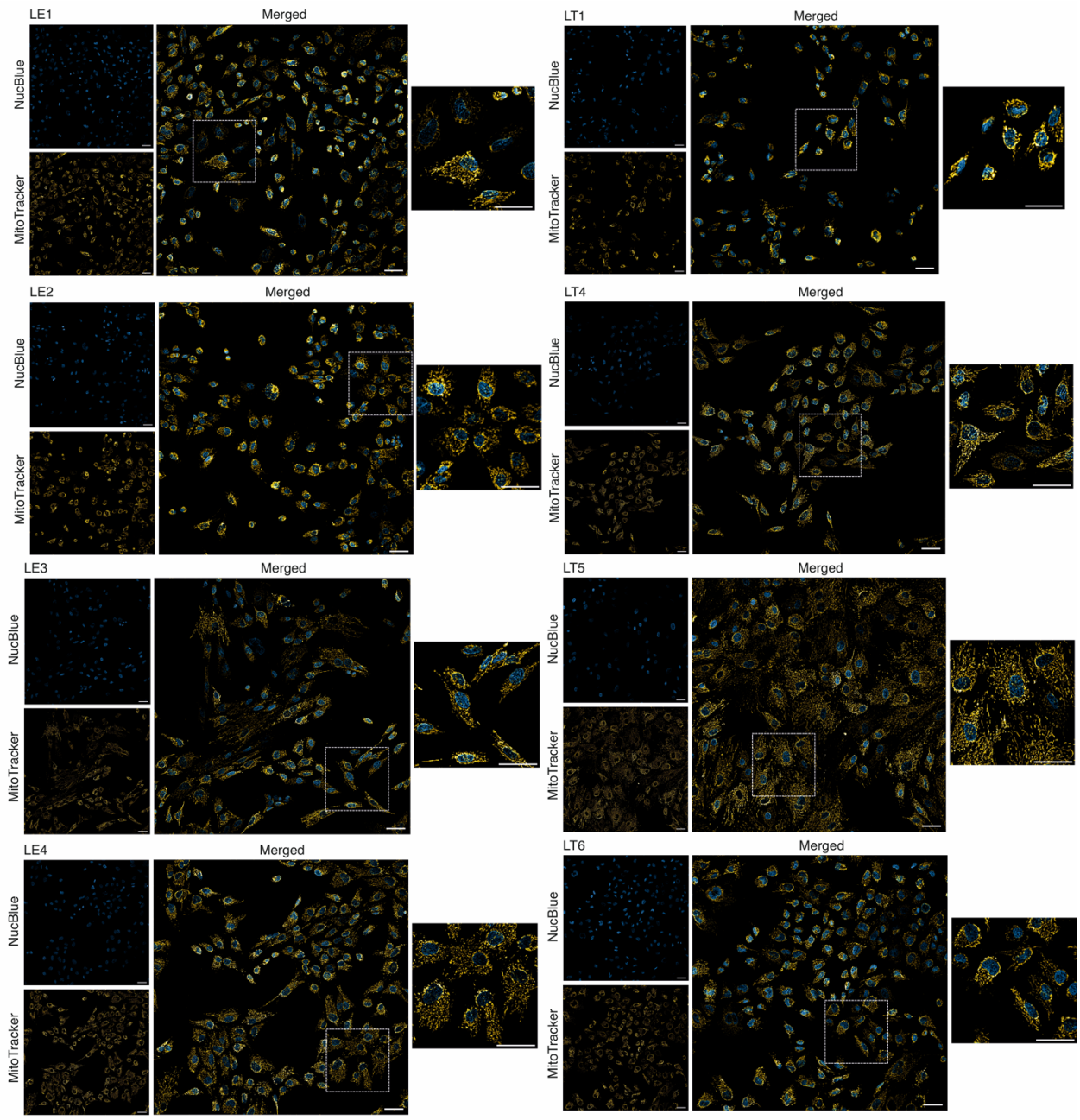

S-Fig. 7. Morphological comparisons of the cell lines. Squared inset image reproduced in Fig. 6 of the main article. Blue: nuclei stain, yellow: mitochondrial stain. All scale bars 50 µm.

MOLECULAR ECOLOGY

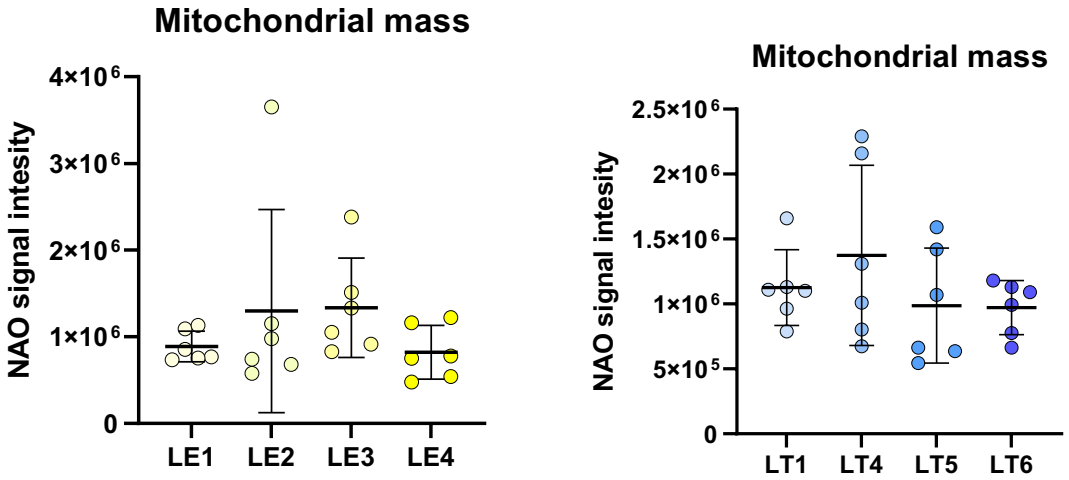

S-Fig. 8. Mitochondrial mass per cell line. No significant differences. One-way ANOVA. LE = *Lepus europaeus*, LT = *Lepus timidus*.

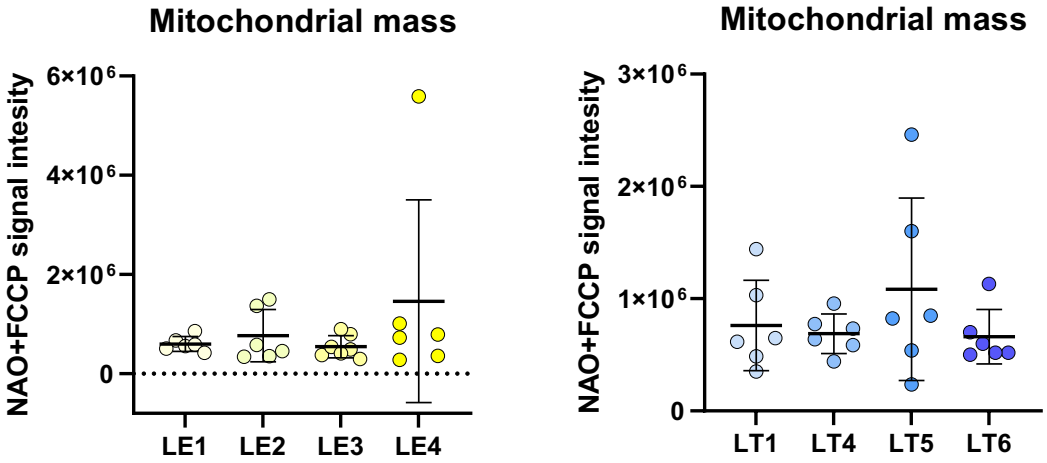

S-Fig. 9. Mitochondrial mass measurement per cell line after addition of uncoupler (FCCP). One-way ANOVA. LE = *Lepus europaeus*, LT = *Lepus timidus*.

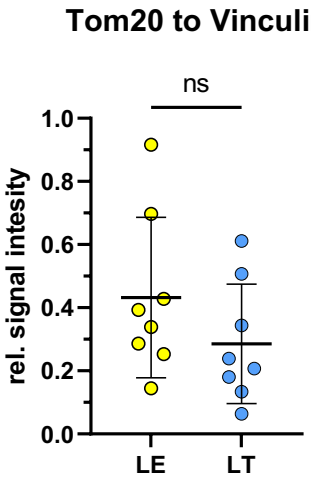

S-Fig. 10. TOM20 levels between the species. Normalized to Vinculin. Species effect: p = 0.058. LE = *Lepus europaeus*, LT = *Lepus timidus*.

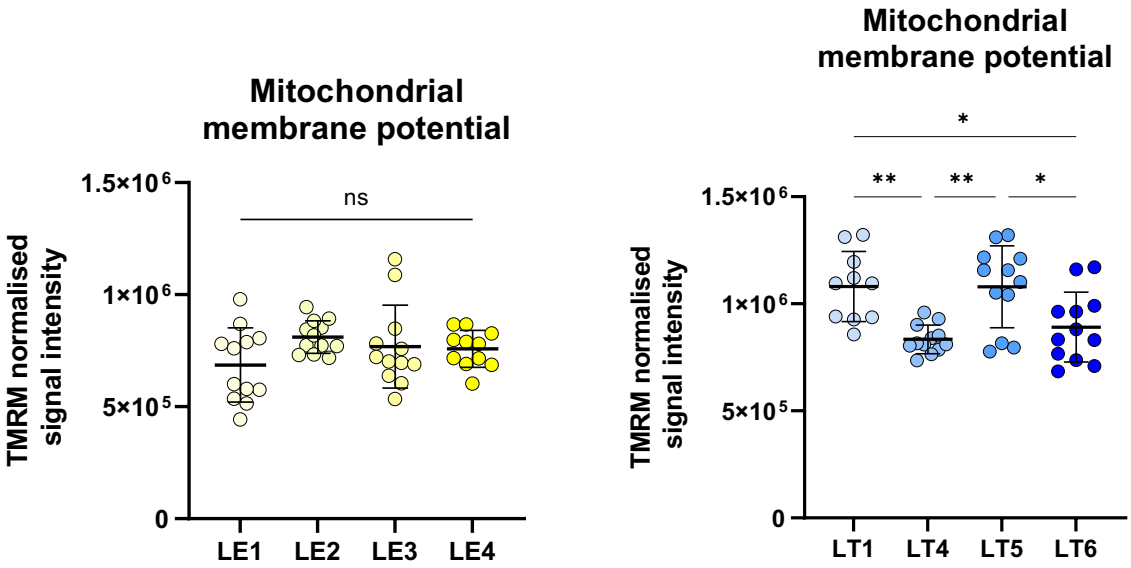

S-Fig. 11. Mitochondrial membrane potential per cell line. * p <0.05, ** p<0.01. One-way ANOVA. LE = *Lepus europaeus*, LT = *Lepus timidus*.